

Test of the universality of τ and μ lepton couplings in W-boson decays with the ATLAS detector

Article (Published Version)

Abraham, N L, Allbrooke, B M M, Aparo, M A, Asquith, L, Cerri, A, De Santo, A, Evans, M O, Grandi, M, Jones, S D, Kelsey, D, Koeck, D M, Safarzadeh Samani, B, Salvatore, F, Shaw, K, Spina, M et al. (2021) Test of the universality of τ and μ lepton couplings in W-boson decays with the ATLAS detector. *Nature Physics*, 17 (7). pp. 813-818. ISSN 1745-2473

This version is available from Sussex Research Online: <http://sro.sussex.ac.uk/id/eprint/101177/>

This document is made available in accordance with publisher policies and may differ from the published version or from the version of record. If you wish to cite this item you are advised to consult the publisher's version. Please see the URL above for details on accessing the published version.

Copyright and reuse:

Sussex Research Online is a digital repository of the research output of the University.

Copyright and all moral rights to the version of the paper presented here belong to the individual author(s) and/or other copyright owners. To the extent reasonable and practicable, the material made available in SRO has been checked for eligibility before being made available.

Copies of full text items generally can be reproduced, displayed or performed and given to third parties in any format or medium for personal research or study, educational, or not-for-profit purposes without prior permission or charge, provided that the authors, title and full bibliographic details are credited, a hyperlink and/or URL is given for the original metadata page and the content is not changed in any way.



OPEN

Test of the universality of τ and μ lepton couplings in W -boson decays with the ATLAS detector

ATLAS Collaboration*

The standard model of particle physics encapsulates our best current understanding of physics at the smallest scales. A fundamental axiom of this theory is the universality of the couplings of the different generations of leptons to the electroweak gauge bosons. The measurement of the ratio of the decay rate of W bosons to τ leptons and muons, $R(\tau/\mu)$, constitutes an important test of this axiom. Using 139 fb^{-1} of proton-proton collisions recorded with the ATLAS detector at a centre-of-mass energy of 13 TeV , we report a measurement of this quantity from di-leptonic $t\bar{t}$ events where the top quarks decay into a W boson and a bottom quark. We can distinguish muons originating from W bosons and those originating from an intermediate τ lepton through the muon transverse impact parameter and differences in the muon transverse momentum spectra. The measured value of $R(\tau/\mu)$ is 0.992 ± 0.013 [$\pm 0.007(\text{stat}) \pm 0.011(\text{syst})$] and is in agreement with the hypothesis of universal lepton couplings as postulated in the standard model. This is the only such measurement from the Large Hadron Collider, so far, and obtains twice the precision of previous measurements.

It is a fundamental axiom of the standard model (SM) that the couplings of the electroweak gauge bosons (W , Z) to charged leptons, g_ℓ (ℓ = electron (e), muon (μ), tau (τ)), are independent of the mass of the leptons. This fundamental assumption is referred to as ‘lepton-flavour universality’ and is tested in this Article by comparing the relative decay rates, or branching ratios (B), of on-shell W bosons to τ leptons and muons, by measuring the ratio $R(\tau/\mu) = B(W \rightarrow \tau\nu_\tau)/B(W \rightarrow \mu\nu_\mu)$.

The measurement exploits the large number of top and anti-top quark pair ($t\bar{t}$) events produced in proton-proton (pp) collisions at the Large Hadron Collider (LHC). Given that $B(t \rightarrow Wq)$ is close to 100%, this gives a very large sample of W -boson pairs. These are used to obtain a large sample of clean and unbiased W -boson decays to muons and τ leptons. The τ leptons are identified through their decay to muons. The τ lepton has a significant lifetime^{1,2} compared to the W boson and undergoes a multi-body decay to a muon and neutrinos. This leaves two distinctive signatures in the detector, the displacement of the τ decay vertex and, on average, a lower muon transverse momentum (p_T). These features are used to distinguish between muons from the $W \rightarrow \tau\nu_\tau \rightarrow \mu\nu_\mu\nu_\tau\nu_\tau$ and $W \rightarrow \mu\nu_\mu$ processes, to extract $R(\tau/\mu)$. The precision of the measurement relies on the highly accurate reconstruction of muon tracks obtainable by the ATLAS experiment.

Previously, $R(\tau/\mu)$ has been measured at the Large Electron-Positron Collider (LEP), yielding a combined value of 1.070 ± 0.026 (ref. ³). The SM expectation of $R(\tau/\mu)$ is unity (neglecting very small phase space effects due to the masses of the decay products, $\sim 5 \times 10^{-4}$)⁴, which differs from the measured value, motivating a precise measurement of this ratio at the LHC. Other experimental measurements of the ratio $B(W \rightarrow \tau\nu_\tau)/B(W \rightarrow \ell\nu_\ell)$, where ℓ is either an electron or a muon, have not yet reached the precision of the LEP results^{5–9}. The equivalent ratio for the two light generations, $B(W \rightarrow \mu\nu_\mu)/B(W \rightarrow e\nu_e)$, has been accurately measured by the LEP³, LHCb¹⁰ and ATLAS¹¹ experiments, and is found to be consistent with the SM prediction at the 1% level. Additionally, although most low-energy experiments¹² show good agreement, to very high precision, with the hypothesis of universality of lepton couplings, recent

results from LHCb^{13–16}, Belle^{17–19} and BaBar^{20,21} show some tension with the SM, further motivating this analysis.

This measurement relies on precise knowledge of the branching ratio of τ leptons decaying to muons to extrapolate to the full $W \rightarrow \tau\nu_\tau$ branching ratio. The value of $(17.39 \pm 0.04)\%$, measured by the LEP experiments^{4,22–25}, is used in the analysis.

Experimental set-up

The ATLAS experiment^{26–28} at the LHC is a multipurpose particle detector with nearly hermetic coverage for recording particles produced in LHC collisions through a combination of particle position and energy measurements. ATLAS has a forward-backward symmetric cylindrical geometry and a near 4π coverage in solid angle. More details of the ATLAS coordinate system are provided in the Methods. ATLAS consists of an inner tracking detector surrounded by a thin superconducting solenoid providing an axial magnetic field of 2 T, electromagnetic and hadron calorimeters, and a muon spectrometer. The inner tracking detector covers the pseudorapidity range $|\eta| < 2.5$. It consists of silicon pixel, silicon microstrip, and transition radiation tracking detectors, and the innermost layer of the pixel detector is at a radius of 33 mm from the beamline, providing a precise measurement of track impact parameters. Lead/liquid-argon (LAr) sampling calorimeters provide electromagnetic energy measurements with high granularity. A steel/scintillator-tile hadron calorimeter covers the central pseudorapidity range ($|\eta| < 1.7$). The endcap and forward regions of the detector are instrumented with LAr calorimeters for both electromagnetic and hadronic energy measurements up to $|\eta| = 4.9$. The muon spectrometer surrounds the calorimeters and is based on three large air-core toroidal superconducting magnets with eight coils each. The field integral of the toroids ranges between 2.0 and 6.0 T m across most of the detector. The muon spectrometer includes a system of precision tracking chambers and fast detectors for triggering. A two-level trigger system is used to select events. The first-level trigger is implemented in hardware and uses a subset of the detector information to accept events at a rate of 100 kHz. This is followed by a software-based trigger that reduces

*A list of authors and their affiliations appears online.

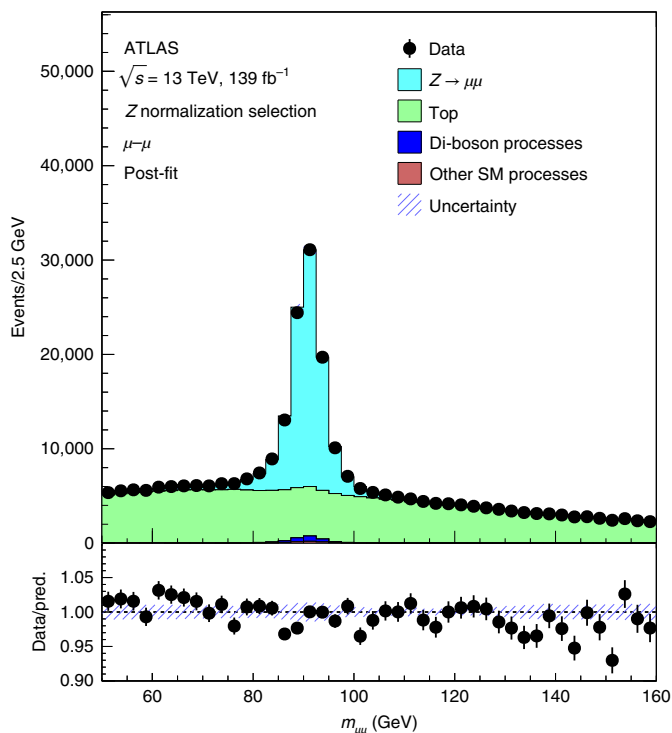


Fig. 1 | $Z \rightarrow \mu\mu$ background normalization. A region enriched in $Z \rightarrow \mu\mu$ events is defined by selecting events with two muons. This control region is used to extract the $Z \rightarrow \mu\mu$ normalization, which is applied in the signal region. A histogram with a fixed bin width of 2.5 GeV of the di-muon invariant mass ($m_{\mu\mu}$) distribution is shown in the figure. The data are shown by black markers and the different components contributing to this region, taken from simulation, are shown by stacked histograms. The different contributions are the primary process of interest ($Z \rightarrow \mu\mu$), along with the main backgrounds from events involving top quarks (Top), a pair of W and/or Z bosons (Di-boson processes) and the grouping of all remaining SM processes (Other SM processes). The bottom panel shows the ratio of the data to the predicted expectation after the fit. The uncertainties on the data are the Poisson errors due to the limited size of the data sample. Blue bands indicate the $\pm 1\sigma$ systematic uncertainties on the prediction, with the constraints from the analysis fit applied.

the accepted event rate to 1 kHz, on average, depending on the data-taking conditions.

The analysed pp collision data were recorded with the ATLAS detector from 2015 to 2018 at a centre-of-mass energy of $\sqrt{s} = 13$ TeV. Owing to the conditions required to achieve high instantaneous luminosity, in these data there are additional collisions in the same and neighbouring LHC proton bunch crossings (pile-up). This resulted in an average of 34 collisions per bunch crossing.

Events in this measurement were selected by single-lepton triggers^{29–31} requiring a single high- p_T isolated electron or muon. After the application of data-quality requirements³², the data sample corresponds to an integrated luminosity of 139 fb^{-1} with an uncertainty of 1.7%³³, obtained using the LUCID-2 detector³⁴ for the primary luminosity measurements.

Samples of simulated events were produced using Monte Carlo techniques to model the different SM processes. After event generation of the process of interest for each sample, the detector response was modelled using a simulation based on GEANT4³⁵. The data and Monte Carlo simulated events were passed through the same reconstruction and analysis procedures. Samples were simulated for the

signal processes, the production of $t\bar{t}$ and single top quarks in association with a W boson (Wt), as well as the different backgrounds. Precise details of the theoretical predictions and event generators used to create the simulated events are provided in the Methods.

Selecting a pure and unbiased sample of W bosons

Collisions are selected to obtain a high-purity sample of $t\bar{t}$ events in which the top quarks decay into a W boson and a b quark, and the two W bosons then decay to leptons. This is referred to as di-leptonic $t\bar{t}$. The two leptonic W -boson decays are exploited in a tag and probe approach: in each event, tag leptons (electrons or muons) are used to select the event, after which a test is performed to determine, in an unbiased way, whether the probe muon was directly produced by a W boson, $W \rightarrow \mu\nu_\mu$, or via an intermediate τ lepton, $W \rightarrow \tau\nu_\tau \rightarrow \mu\nu_\mu\nu_\tau$. Events are categorized into signal regions, used to extract $R(\tau/\mu)$, and additional control regions, used to constrain the normalization of the major backgrounds.

The selections rely on reconstructed muons, electrons and hadronic jets. Details of the physics object reconstruction definitions used are provided in the Methods. Events entering the signal region are required to contain either one electron and one muon of opposite electric charge ($e\text{--}\mu$ channel) or two muons of opposite electric charge ($\mu\text{--}\mu$ channel). In the $e\text{--}\mu$ channel, the electron is required to pass the trigger, and in the $\mu\text{--}\mu$ channel, the tag muon is required to pass the trigger. This ensures that the probe muons have no trigger bias. If both leptons in the $\mu\text{--}\mu$ channel satisfy the tag and probe criteria, both muons in turn are used as probes. Events with more than two leptons are rejected. In addition, events must have at least two reconstructed hadronic jets that are identified as containing a b hadron. Finally, to reduce the backgrounds from Z bosons and hadron decays, events where the invariant mass of the two muons, $m_{\mu\mu}$, satisfies $85 < m_{\mu\mu} < 95$ GeV are excluded in the $\mu\text{--}\mu$ channel, and events with di-lepton mass $m_{\ell\ell} < 15$ GeV are excluded in both channels.

This selection results in a sample of approximately half a million collision events, with a di-leptonic $t\bar{t}$ purity of over 95% in the $e\text{--}\mu$ channel and 85% in the $\mu\text{--}\mu$ channel. This sample is used to test the origin of the probe muons and extract the measurement of $R(\tau/\mu)$. This is extracted from the ratio of the number of events in which the probe muon originates from the process $W \rightarrow \tau\nu_\tau \rightarrow \mu\nu_\mu\nu_\tau$, referred to as $\mu_{\tau(\rightarrow\mu)}$, to those that come from the process $W \rightarrow \mu\nu_\mu$, referred to as μ_{prompt} . A fit is performed that exploits the difference in shape between these two components and the backgrounds of the distributions of the probe muon's transverse impact parameter $|d_0^\mu|$ and its transverse momentum p_T^μ .

Muon transverse impact parameter distribution calibration

The muon's transverse impact parameter $|d_0^\mu|$ has particular importance for this analysis and requires careful treatment. It is measured in the $x\text{--}y$ plane as the closest distance of approach of the track to the beamline. The shape of the $|d_0^\mu|$ distribution of prompt muons is determined using a $Z \rightarrow \mu\mu$ calibration region to create templates that are used to predict the distribution in the signal region.

The calibration region is defined by requiring that two muons satisfying the same kinematic criteria as in the signal region, but with the di-muon mass requirement changed to $85 < m_{\mu\mu} < 100$ GeV. No requirements on hadronic jets are applied. This gives a sample of ~ 95 million prompt muons with a purity of $> 99.9\%$.

Templates of the shape of the $|d_0^\mu|$ distribution are then taken from this data sample after subtracting the expected contributions from the simulation of processes with significant muon parent lifetimes, primarily $Z \rightarrow \tau\tau$. These $|d_0^\mu|$ templates are extracted in 33 bins in p_T^μ and $|\eta^\mu|$ to capture the dependence of the distribution on these variables. Separate templates are used for 2015+2016, 2017 and 2018 data to account for differences in the beam conditions and in the alignment of the inner detector.

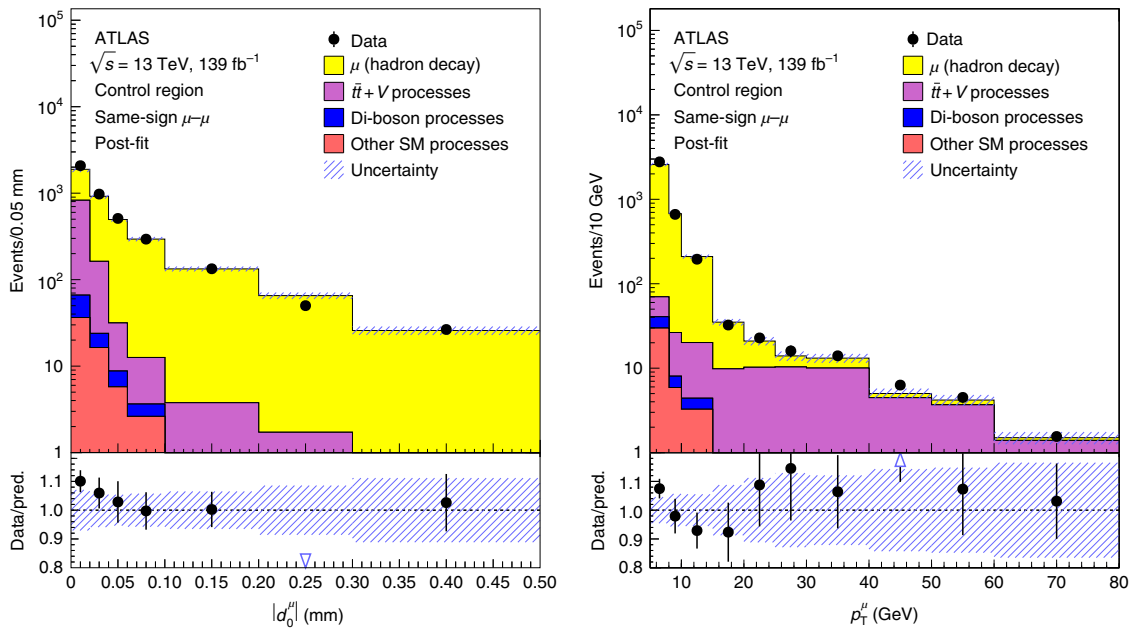


Fig. 2 | μ_{had} background normalization. A region enriched in μ_{had} events is defined by selecting events with two same-sign muons. This control region is used to extract normalization factors to correct the μ_{had} prediction to match the data. The probe muon transverse impact parameter (left, $|d_0^\mu|$) and transverse momentum (right, p_T^μ) distributions in this region are shown. The data are shown by black markers and the different components contributing to this region, taken from simulation, are shown by stacked histograms. The different contributions are the primary process of interest, μ_{had} (μ (hadron decay)), along with the main backgrounds from events involving a top quark pair produced in association with a W or Z boson ($t\bar{t} + V$ processes), a pair of W and/or Z bosons (Di-boson processes) and the grouping of all remaining SM processes (Other SM processes). The y-axis label includes the value that defines the scaling of the variable bin width histogram. The extracted normalization factor is applied to the μ_{had} prediction, along with the effect of any constraints and pulls on the systematic uncertainties from the fit to the signal region data. The bottom panels show the ratio of the data to the predicted expectation after the fit. The uncertainties on the data are the Poisson errors due to the limited size of the data sample. Blue bands indicate the $\pm 1\sigma$ systematic uncertainties on the prediction with the constraints from the analysis fit applied. The open blue arrowheads in the ratio panel indicate points where the ratio values lie outside the y-axis range shown.

Additionally, using this calibration region, the Gaussian part of the $|d_0^\mu|$ resolution is estimated in data and simulation by fitting the $|d_0^\mu|$ distribution in the range $|d_0^\mu| < 0.02$ mm. For $p_T^\mu = 20$ GeV, the resolution is $\sim 14\mu\text{m}$. Corrections to account for differences in the resolution of the detector between the data and simulation are applied to the muons from τ decays and hadron decays. For the range of $|d_0^\mu|$ values considered in this analysis, $|d_0^\mu| < 0.5$ mm, the resolution measured from prompt muons is applicable to those with significant displacement.

Background normalization estimation

The two largest backgrounds are $Z(\rightarrow\mu\mu) + \text{jets}$ and events in which the probe muon does not originate from a W -boson decay. Three dedicated control regions are used to extract the normalization of these backgrounds.

The $Z(\rightarrow\mu\mu) + \text{jets}$ background is important at small values of $|d_0^\mu|$. The normalization of the $Z(\rightarrow\mu\mu) + \text{jets}$ background in the $\mu\text{--}\mu$ channel is extracted from the data in a control region where the same event selection is applied, including the hadronic jet requirements, but without the $m_{\mu\mu}$ criterion, and is then extrapolated to the signal region using simulation. In the control region, the peak of the invariant mass distribution of the di-muon system is fitted over the range $50 < m_{\mu\mu} < 140$ GeV. A Voigt profile³⁶ is used for the $Z \rightarrow \mu\mu$ resonance and a third-order Chebychev polynomial for all non-resonant processes, which provides a good description of the data. Other functions were tested to provide a systematic uncertainty, which is combined with the statistical uncertainties. The normalization factor required to scale the simulated sample to data is found to be 1.36 ± 0.01 . The di-muon invariant mass in the control region is shown in Fig. 1 after this normalization is applied.

This normalization factor is also applied to the small $Z(\rightarrow\tau\tau) + \text{jets}$ background.

The most important background at large values of $|d_0^\mu|$ is from events in which the probe muon originates from the decay of b or c hadrons, or more rarely from in-flight decays of π^\pm and K^\pm . This occurs primarily in $t\bar{t}$ events where one W boson decays leptonically and the other hadronically, referred to as semi-leptonic $t\bar{t}$. These muons are referred to as μ_{had} . A data-driven method is used to determine the normalization of this background from two control regions, one each for the $e\text{--}\mu$ and $\mu\text{--}\mu$ channels. The control regions have the same event selection as the signal regions, but the two leptons are required to have same-sign electric charge. This results in a sample with a high purity of this μ_{had} background. The largest source of μ_{had} is from decays of b hadrons, and this contributes equally to same-sign and opposite-sign selections, while the other substantial source, c hadrons, has a component in both selections, but they are not equal. The extrapolation from same-sign control region to opposite-sign signal region is estimated from simulation. In the same-sign control region there are two backgrounds to μ_{had} at high p_T^μ : $t\bar{t} + V$, and $t\bar{t}$, which occurs through electron charge misidentification in the $e\text{--}\mu$ channel. A normalization correction factor is applied to these processes based on the number of events observed with a probe muon with $p_T^\mu > 30$ GeV. This is done before extracting the normalization of the μ_{had} background. The normalization factors to scale the simulation to data for the μ_{had} background are found to be 1.39 and 1.37 in the $e\text{--}\mu$ and $\mu\text{--}\mu$ channels, respectively. Figure 2 shows that the simulation and data are consistent within uncertainties in the $\mu\text{--}\mu$ channel same-sign control region, providing confidence that the differential distributions of p_T^μ and $|d_0^\mu|$ are well-modelled.

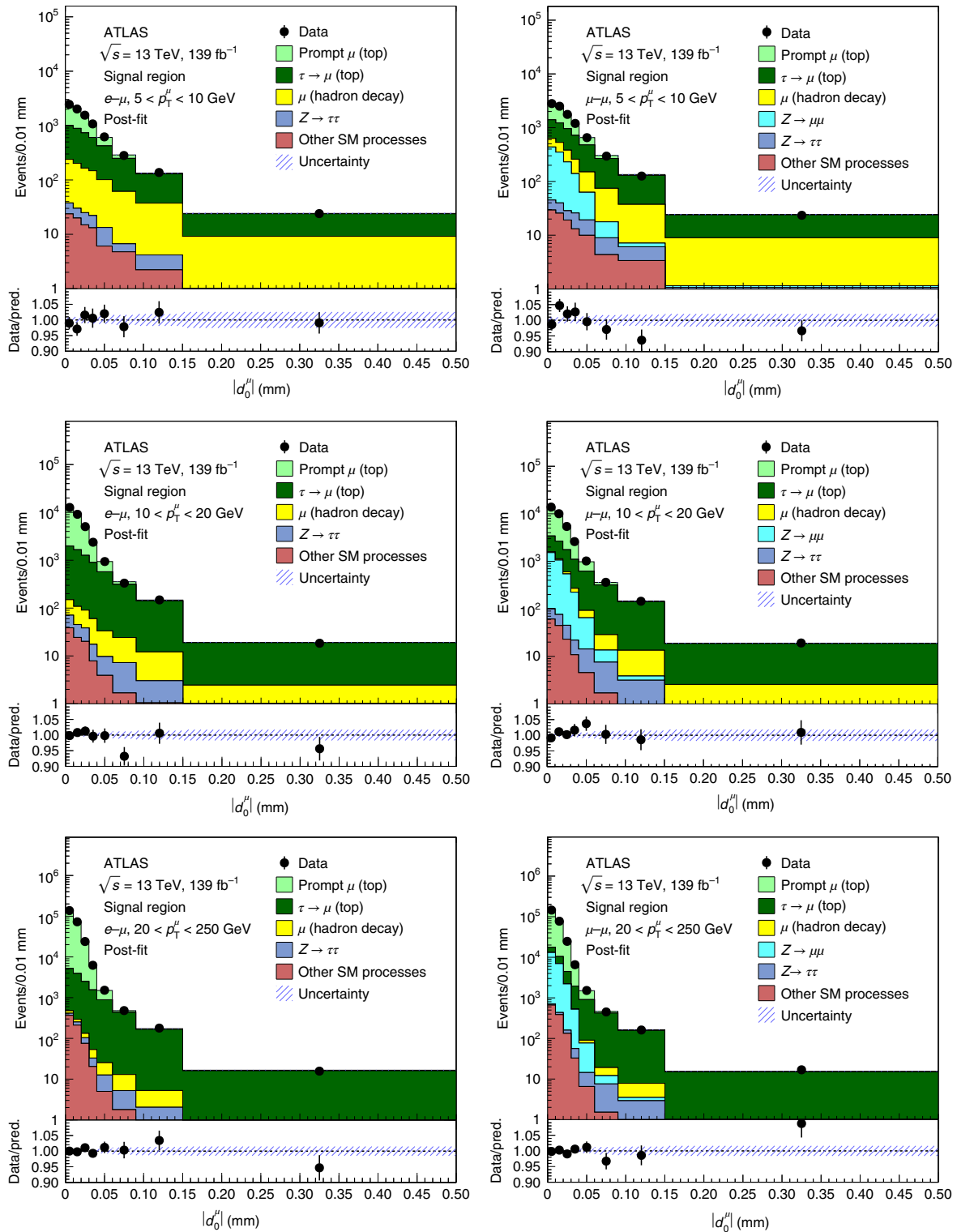


Fig. 3 | Transverse impact parameter distributions of probe muons in the signal region. The signal region used to extract $R(\tau/\mu)$ is enriched in di-lepton $t\bar{t}$ events. The $|d_0^\mu|$ distributions for each signal region (left, $e-\mu$ channel; right, $\mu-\mu$ channel) and probe muon p_T^μ bin (top, $5 < p_T^\mu < 10$ GeV; middle, $10 < p_T^\mu < 20$ GeV; bottom, $20 < p_T^\mu < 250$ GeV) used in the analysis are shown. The data are represented by black markers and the different components contributing to this region, taken from simulation, are shown by stacked histograms. The different contributions are the two primary processes of interest used to extract $R(\tau/\mu)$, μ_{prompt} from top quark decays (Prompt μ (top)) and $\mu_{\tau \rightarrow \mu}$ from top decays ($\tau \rightarrow \mu$ (top)). The main backgrounds are also shown: events with a μ_{had} (μ (hadron decay)), events with a Z boson decaying to a di-muon pair ($Z \rightarrow \mu\mu$), events with a Z boson decaying to a di- τ pair ($Z \rightarrow \tau\tau$) and the grouping of all remaining SM processes (Other SM processes). Distributions are shown after the fit has been performed. The y-axis label includes the value that defines the scaling of the variable bin width histogram. The bottom panels show the ratio of the data to the predicted expectation after the fit. The uncertainties on the data are the Poisson errors due to the limited size of the data sample. Blue bands indicate the $\pm 1\sigma$ systematic uncertainties on the prediction with the constraints from the analysis fit applied. The contribution from ‘Other SM processes’ is dominated by di-boson and $t\bar{t} + V$ production. The chi-squared statistic values range from 3.5 to 10.2 for eight degrees of freedom for the distributions.

Table 1 | Sources of uncertainty

Source	Impact on $R(\tau/\mu)$
Prompt d_0^μ templates	0.0038
μ_{prompt} and $\mu_{\tau(\rightarrow\mu)}$ parton shower variations	0.0036
Muon isolation efficiency	0.0033
Muon identification and reconstruction	0.0030
μ_{had} normalization	0.0028
$t\bar{t}$ scale and matching variations	0.0027
Top p_T spectrum variation	0.0026
μ_{had} parton shower variations	0.0021
Monte Carlo statistics	0.0018
Pile-up	0.0017
$\mu_{\tau(\rightarrow\mu)}$ and μ_{had} d_0^μ shape	0.0017
Other detector systematic uncertainties	0.0016
Z+jet normalization	0.0009
Other sources	0.0004
$B(\tau \rightarrow \mu\nu_\tau\nu_\mu)$	0.0023
Total systematic uncertainty	0.0109
Data statistics	0.0072
Total	0.013

The main sources of uncertainty on the measured value of $R(\tau/\mu)$ are shown. The size of the impact each uncertainty has on $R(\tau/\mu)$ is assessed by fixing the relevant fit parameters for a given uncertainty and refitting to data. The reduction in the total uncertainty in this modified fit gives the quoted impact. Different individual components used in the fit are combined into categories.

Fit configuration and systematic uncertainties

A two-dimensional profile likelihood fit³⁷ is performed in the $|d_0^\mu|$ and p_T^μ distributions. The bin boundaries were chosen to provide the best separation between the different μ_{prompt} , $\mu_{\tau(\rightarrow\mu)}$ and μ_{had} processes given the available data. This resulted in three bins in p_T^μ (boundaries of 5, 10, 20 and 250 GeV) and eight bins in the transverse impact parameter $|d_0^\mu|$ (boundaries of 0, 0.01, 0.02, 0.03, 0.04, 0.06, 0.09, 0.15 and 0.5 mm), of the probe muon for both the $e-\mu$ and $\mu-\mu$ channels, making 48 bins in total.

The ratio of the number of $\mu_{\tau(\rightarrow\mu)}$ events to the number μ_{prompt} is fitted by minimizing the negative log-likelihood, to measure $R(\tau/\mu)$. More than 100 (nuisance) parameter values representing the statistical and systematic uncertainties, which can be modified by the fit, are included. The relative uncertainty of 0.23% in the $\tau \rightarrow \mu\nu_\mu\nu_\tau$ branching ratio is also included in the measured value of $R(\tau/\mu)$ and is a subdominant component of the overall uncertainty. As both the $t\bar{t}$ and Wt processes contain two W bosons, both are treated as signal. Two fit parameters are allowed to float freely: $R(\tau/\mu)$ and $k(t\bar{t})$. The $k(t\bar{t})$ parameter is a constant scaling factor applied to the normalization of both the μ_{prompt} and $\mu_{\tau(\rightarrow\mu)}$ components of the signal, whereas $R(\tau/\mu)$ only affects the $\mu_{\tau(\rightarrow\mu)}$ components. Both are applied across all bins and in both channels. $R(\tau/\mu)$ is the parameter of interest and is not affected by the overall normalization scaling factors of the $t\bar{t}$ and Wt processes. The fit is performed after applying the normalization scaling factors derived in the control regions. Other processes are normalized to their theoretical cross-sections, taking into account the uncertainty in these predictions.

Because many systematic uncertainties are correlated between the μ_{prompt} and $\mu_{\tau(\rightarrow\mu)}$ templates, they cancel out in the $R(\tau/\mu)$ ratio, minimizing their impact on the precision of the result. These include uncertainties related to jet reconstruction, flavour tagging and trigger efficiencies. The remaining dominant uncertainties are the uncertainties in the data-driven methods, the theoretical modelling uncertainties and the reconstruction uncertainties; these

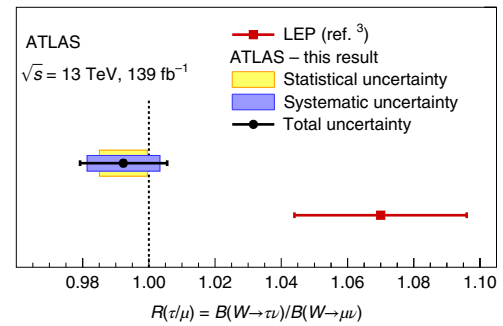


Fig. 4 | Summary of ATLAS and LEP results. The new ATLAS measurement of $R(\tau/\mu)$ and the previous LEP result³ of the same quantity. The new measurement from ATLAS is shown by the black filled circle and the LEP result by a red filled square. For the ATLAS result the statistical (yellow box) and systematic (blue box) errors are shown separately, along with the total error of the measurement (black bars). The total uncertainty on the LEP result is indicated by the red bars. The vertical dashed line indicates the prediction lepton-flavour universality of the SM, with equal W -boson branching ratios to different lepton flavours.

are described in the following and further details are provided in the Methods.

An uncertainty associated with the data-driven templates for the $|d_0^\mu|$ distribution of μ_{prompt} is derived to account for the differences between the $Z \rightarrow \mu\mu$ calibration region where they were derived and the signal region.

Uncertainties in the data-driven normalization of the μ_{had} background due to the size of the same-sign dataset, the choice of Monte Carlo generators used and the uncertainty in the subtraction of the other processes in the same-sign control region are included in the fit. The uncertainties associated with the Z+jets normalization derived from data are also applied. Uncertainties on the cross-section calculations and the integrated luminosity are applied to all other backgrounds estimated from simulation, but have a minor impact on the result.

Uncertainties in the shape of the μ_{prompt} , $\mu_{\tau(\rightarrow\mu)}$ and μ_{had} distributions due to the modelling of the simulated $t\bar{t}$ samples are derived. The combined yield of the μ_{prompt} and $\mu_{\tau(\rightarrow\mu)}$ templates is allowed to float in the fit, but changes in generator configuration choices can result in modifications to the muon p_T^μ and subsequently the $|d_0^\mu|$ distribution, such that there can be relative changes in the μ_{prompt} and $\mu_{\tau(\rightarrow\mu)}$ template yields in each bin, leading to an uncertainty in $R(\tau/\mu)$. For the μ_{had} background, in addition to the uncertainties in the normalization, there can be changes to the muon p_T^μ modelling and the relative fractions of muons from different sources, both of which can change the shape of the $|d_0^\mu|$ distribution. The most important of these variations is in the parton shower and hadronization model.

The muon reconstruction and isolation efficiencies are determined in di-muon ($Z \rightarrow \mu\mu$ and $J/\psi \rightarrow \mu\mu$) data and simulation using a tag and probe method³⁸. Corrections are applied to the simulated samples to account for the differences between data and simulation, and the uncertainties on these correction factors are included in the analysis. Additionally, an uncertainty due to the modelling of pile-up is obtained by reweighting the simulated events³⁹.

Extraction of $R(\tau/\mu)$

Figure 3 shows the differential distributions of $|d_0^\mu|$ in the six signal regions for the data and the expectation after the fit to data. Good agreement is observed between the corrected simulation samples and the data. The global goodness of fit when fitting the expectation from simulation, defined as twice the change in negative

log-likelihood relative to a fit performed assuming the pre-fit expectation per degree of freedom, has a value of 1.11 (P value of 0.29).

The separation between the μ_{prompt} and $\mu_{\tau(\rightarrow\mu)}$ processes can be seen clearly. The μ_{prompt} processes dominate at low $|d_0^\mu|$, whereas $\mu_{\tau(\rightarrow\mu)}$ dominates at high $|d_0^\mu|$. The μ_{had} background is also important at high $|d_0^\mu|$, but contributes most significantly at low p_T^μ .

The analysis was finalised before looking at the value of $R(\tau/\mu)$ in the data to minimize any bias. It was also checked that the result is consistent with respect to different channels, kinematic bins, data-taking periods and the charge of the probe lepton.

The total systematic uncertainty is 0.011, including the uncertainty in the $\tau \rightarrow \mu\nu_\tau\nu_\tau$ branching ratio, and the statistical uncertainty is 0.007. Table 1 lists the different contributions of systematic uncertainty grouped into categories. The leading contributions come from the imperfect knowledge of the tail of the $|d_0^\mu|$ distribution, the parton shower and hadronization model uncertainty, and the muon selection uncertainties.

The measured value of $R(\tau/\mu)$ is

$$R(\tau/\mu) = 0.992 \pm 0.013 [\pm 0.007 (\text{stat}) \pm 0.011 (\text{syst})],$$

exceeding the precision from LEP which measured 1.070 ± 0.026 . The result is shown in Fig. 4 alongside the combination of LEP measurements. The present result agrees with the SM expectation of equal couplings for different lepton flavours and the hypothesis of lepton-flavour universality.

This result surpasses the precision of the previous LEP result and resolves the tension they observed with the SM prediction of lepton-flavour universality. This precise measurement of $R(\tau/\mu)$ achieved so far, this is an example of the ability of the ATLAS experiment to perform high-precision measurements.

Online content

Any methods, additional references, Nature Research reporting summaries, source data, extended data, supplementary information, acknowledgements, peer review information; details of author contributions and competing interests; and statements of data and code availability are available at <https://doi.org/10.1038/s41567-021-01236-w>.

Received: 28 July 2020; Accepted: 30 March 2021;
Published online: 5 July 2021

References

- Feldman, G. J. et al. Measurement of the τ lifetime. *Phys. Rev. Lett.* **48**, 66–69 (1982).
- Belle Collaboration Measurement of the τ -lepton lifetime at Belle. *Phys. Rev. Lett.* **112**, 031801 (2014).
- LEP Electroweak Working Group Electroweak measurements in electron–positron collisions at W -boson-pair energies at LEP. *Phys. Rep.* **532**, 119–244 (2013).
- Particle Data Group Review of particle physics. *Phys. Rev. D* **98**, 030001 (2018).
- UA1 Collaboration Studies of intermediate vector boson production and decay in UA1 at the CERN proton–antiproton collider. *Z. Phys. C* **44**, 15–61 (1989).
- CDF Collaboration Measurement of the ratio $B(W \rightarrow \tau\nu)/B(W \rightarrow e\nu)$ in $p\bar{p}$ collisions at $\sqrt{s}=1.8$ TeV. *Phys. Rev. Lett.* **68**, 3398–3402 (1992).
- UA2 Collaboration A search for charged Higgs from top quark decay at the CERN $p\bar{p}$ collider. *Phys. Lett. B* **280**, 137–145 (1992).
- D0 Collaboration Measurement of the $W \rightarrow \tau\nu$ production cross section in $p\bar{p}$ collisions at $\sqrt{s}=1.8$ TeV. *Phys. Rev. Lett.* **84**, 5710–5715 (2000).
- CMS Collaboration Measurement of the top quark pair production cross section in dilepton final states containing one τ lepton in pp collisions at $\sqrt{s}=13$ TeV. *J. High Energy Phys.* **02**, 191 (2020).
- LHCb Collaboration Measurement of forward $W \rightarrow e\nu$ production in pp collisions at $\sqrt{s}=8$ TeV. *J. High Energy Phys.* **10**, 030 (2016).
- ATLAS Collaboration Precision measurement and interpretation of inclusive W^+ , W^- and Z/γ^* production cross sections with the ATLAS detector. *Eur. Phys. J. C* **77**, 367 (2017).
- Pich, A. Precision tau physics. *Prog. Part. Nucl. Phys.* **75**, 41–85 (2014).
- LHCb Collaboration Measurement of the ratio of the $B^0 \rightarrow D^-\tau^+\nu_\tau$ and $B^0 \rightarrow D^-\mu^+\nu_\mu$ branching fractions using three-prong τ -lepton decays. *Phys. Rev. Lett.* **120**, 171802 (2018).
- LHCb Collaboration Test of lepton flavor universality by the measurement of the $B^0 \rightarrow D^*\tau^+\nu_\tau$ branching fraction using three-prong τ decays. *Phys. Rev. D* **97**, 072013 (2018).
- LHCb Collaboration Measurement of CP-averaged observables in the $B^0 \rightarrow K^0\mu^+\mu^-$ decay. *Phys. Rev. Lett.* **125**, 011802 (2020).
- LHCb Collaboration Angular analysis of the $B^0 \rightarrow K^0\mu^+\mu^-$ decay using 3fb^{-1} of integrated luminosity. *J. High Energy Phys.* **02**, 104 (2016).
- Belle Collaboration Measurement of the τ lepton polarization and $R(D')$ in the decay $\bar{B} \rightarrow D^*\tau^-\bar{\nu}_\tau$. *Phys. Rev. Lett.* **118**, 211801 (2017).
- Belle Collaboration Measurement of the τ lepton polarization and $R(D')$ in the decay $\bar{B} \rightarrow D^*\tau^-\bar{\nu}_\tau$ with one-prong hadronic τ decays at Belle. *Phys. Rev. D* **97**, 012004 (2018).
- Belle Collaboration Measurement of $\mathcal{R}(D)$ and $\mathcal{R}(D^*)$ with a semileptonic tagging method. Preprint at <https://arxiv.org/pdf/1904.08794.pdf> (2019).
- BaBar Collaboration Evidence for an excess of $\bar{B} \rightarrow D^{(*)}\tau^-\bar{\nu}_\tau$ decays. *Phys. Rev. Lett.* **109**, 101802 (2012).
- BaBar Collaboration Measurement of an excess of $\bar{B} \rightarrow D^{(*)}\tau^-\bar{\nu}_\tau$ decays and implications for charged Higgs bosons. *Phys. Rev. D* **88**, 072012 (2013).
- ALEPH Collaboration Branching ratios and spectral functions of τ decays: final ALEPH measurements and physics implications. *Phys. Rep.* **421**, 191–284 (2005).
- OPAL Collaboration A measurement of the $\tau \rightarrow \mu\bar{\nu}_\mu\nu_\tau$ branching ratio. *Phys. Lett. B* **551**, 35–48 (2003).
- L3 Collaboration Measurement of the τ branching fractions into leptons. *Phys. Lett. B* **507**, 47–60 (2001).
- DELPHI Collaboration Measurements of the leptonic branching fractions of the tau. *Eur. Phys. J. C* **10**, 201–218 (1999).
- ATLAS Collaboration The ATLAS experiment at the CERN Large Hadron Collider. *J. Instrum.* **3**, S08003 (2008).
- ATLAS Collaboration ATLAS Insertable B-Layer Technical Design Report CERN-LHCC-2010-013, ATLAS-TDR-19 (CERN, 2010); <https://cds.cern.ch/record/1291633>
- Abbott, B. et al. Production and integration of the ATLAS insertable B-layer. *J. Instrum.* **13**, T05008 (2018).
- ATLAS Collaboration Performance of the ATLAS trigger system in 2015. *Eur. Phys. J. C* **77**, 317 (2017).
- ATLAS Collaboration Performance of electron and photon triggers in ATLAS during LHC run 2. *Eur. Phys. J. C* **80**, 47 (2020).
- ATLAS Collaboration Performance of the ATLAS muon triggers in run 2. *J. Instrum.* **15**, P09015 (2020).
- ATLAS Collaboration ATLAS data quality operations and performance for 2015–2018 data-taking. *J. Instrum.* **15**, P04003 (2020).
- ATLAS Collaboration Luminosity Determination in pp Collisions at $\sqrt{s}=13$ TeV using the ATLAS Detector at the LHC (CERN, 2019); <https://cds.cern.ch/record/2677054>
- Avoni, G. et al. The new LUCID-2 detector for luminosity measurement and monitoring in ATLAS. *J. Instrum.* **13**, P07017 (2018).
- Agostinelli, S. et al. GEANT4—a simulation toolkit. *Nucl. Instrum. Methods A* **506**, 250–303 (2003).
- Voigt, W. Über das Gesetz der Intensitätsverteilung Innerhalb der Linien eines Gasspektrums. *Sitzungsberichte* **1914**, 25 (1912).
- Cowan, G. et al. Asymptotic formulae for likelihood-based tests of new physics. *Eur. Phys. J. C* **71**, 1554 (2011); erratum **73**, 2501 (2013).
- ATLAS Collaboration Muon reconstruction performance of the ATLAS detector in proton–proton collision data at $\sqrt{s}=13$ TeV. *Eur. Phys. J. C* **76**, 292 (2016).
- ATLAS Collaboration The Pythia 8 A3 Tune Description of ATLAS Minimum Bias and Inelastic Measurements Incorporating the Donnachie–Landshoff Diffractive Model (CERN, 2016); <https://cds.cern.ch/record/2206965>

Publisher's note Springer Nature remains neutral with regard to jurisdictional claims in published maps and institutional affiliations.



Open Access This article is licensed under a Creative Commons Attribution 4.0 International License, which permits use, sharing, adaptation, distribution and reproduction in any medium or format, as long as you give appropriate credit to the original author(s) and the source, provide a link to the Creative Commons license, and indicate if changes were made. The images or other third party material in this article are included in the article's Creative Commons license, unless indicated otherwise in a credit line to the material. If material is not included in the article's Creative Commons license and your intended use is not permitted by statutory regulation or exceeds the permitted use, you will need to obtain permission directly from the copyright holder. To view a copy of this license, visit <http://creativecommons.org/licenses/by/4.0/>.

© The Author(s) 2021

Methods

ATLAS coordinate system and nomenclature. ATLAS uses a right-handed coordinate system with its origin at the nominal interaction point (IP) in the centre of the detector and the z axis along the beam pipe. The x axis points from the IP to the centre of the LHC ring, and the y axis points upwards. Cylindrical coordinates (r, ϕ) are used in the transverse plane, ϕ being the azimuthal angle around the z axis. The pseudorapidity is defined in terms of the polar angle θ as $\eta = -\ln \tan(\theta/2)$. Angular distance is measured in units of $\Delta R \equiv \sqrt{(\Delta\eta)^2 + (\Delta\phi)^2}$.

The beamline is the central (x - y) axis of the luminous region. The transverse impact parameter, $|d_0^\mu|$, is measured in the x - y plane as the closest distance of approach of the track to the beamline. It is defined relative to the beamline rather than the primary vertex so that the resolution of $|d_0^\mu|$ is independent of the vertex (x - y) resolution, which depends on the physics process.

Monte Carlo simulation and theoretical predictions. The top-pair and single-top-quark events, including Wt -, t - and s -channel production, were generated using the POWHEGBOX^{40–44} generator interfaced to the PYTHIA8^{45–47} parton shower and hadronization model (more details are available in ref. ⁴⁸). The decays of bottom and charm hadrons are important for backgrounds in the analysis and were modelled using the EvtGen⁴⁹ program. The $t\bar{t}$ and single-top processes were normalized to the inclusive cross-section calculation of the highest available precision^{50–58} and $t\bar{t}$ events additionally have a differential reweighting applied to match the next-to-next-to-leading order (NNLO) in quantum chromodynamics (QCD) top quark p_T calculation⁵⁹. For single-top quark production in the Wt channel, the diagram removal scheme⁶⁰ was used to remove overlap with $t\bar{t}$ production. The $t\bar{t} + W$ and $t\bar{t} + Z$ events were simulated with Sherpa and MadGraph5_aMC@NLO⁶¹ interfaced with Pythia8, respectively. The background from $V(W, Z)$ + jets and VV + jets events was simulated with the Sherpa^{44,62–71} generator (more details can be found in refs. ^{72,73}). All processes were normalized to their highest-order available cross-sections^{74,75}.

Simulated inelastic pp collisions³⁹ were overlaid on events in all samples to model the observed data distribution of pile-up from additional collisions in the same and neighbouring bunch crossings.

Object identification in ATLAS. Muons are reconstructed using combined fits of inner detector^{76,77} and muon spectrometer tracks³⁸. They are required to satisfy the ‘medium’ identification criteria of ref. ³⁸. They are also required to be strictly isolated from other activity by requiring that the sum of the p_T of other tracks within a surrounding cone of size $\Delta R = 0.3$ and the sum of p_T calculated from calorimeter energy deposits within a cone of size $\Delta R = 0.2$ around the muons are below certain thresholds. Tag muons are required to have $p_T^\mu > 27.3$ GeV to pass the trigger thresholds, while probe muons are required to have $p_T^\mu > 5$ GeV. Both the tag and probe muons are required to have $|\eta| < 2.5$ and to originate close to the primary vertex with a distance of closest approach in the r - z plane of less than 0.3 mm and a transverse impact parameter relative to the beamline, $|d_0^\mu|$, of less than 0.5 mm. The primary vertex is defined as the vertex with the highest Σp_T^2 of the tracks associated with it. Additional criteria are applied to test the compatibility of the momenta measured separately in the inner detector and the muon spectrometer, to remove reconstructed muons that result from in-flight decays of charged kaons and pions.

Electrons are reconstructed from inner detector tracks matched to clusters of calorimeter-cell energy clusters⁷⁸. They are required to satisfy the ‘tight’ identification criteria of ref. ⁷⁸ and the same strict isolation criteria as applied to muons. Tag electrons are required to have $p_T^e > 27$ GeV to pass the trigger requirements and satisfy $|\eta| < 2.47$, excluding the transition region between the barrel and end-cap calorimeter, $1.37 < |\eta| < 1.52$. They must also satisfy the same criteria as for muons for their distance of closest approach to the primary vertex in the transverse and r - z plane.

Hadronic jets are built from the energy in calorimeter cells at the electromagnetic energy scale⁷⁹, using the anti- k_t algorithm⁸⁰ with a radius parameter of 0.4. They are then calibrated to the energy scale of jets created from stable generator-level particles excluding muons and neutrinos, using the same jet algorithm⁸¹. For jets with $25 < p_T < 60$ GeV and $|\eta| < 2.4$, pile-up suppression requirements in the form of a jet vertex tagger⁸² are applied. Only jets with $p_T > 25$ GeV and $|\eta| < 2.5$ are considered in the analysis. To classify jets as containing a b hadron, the 70% efficiency working point of the MV2c10 b -tagging algorithm^{83,84} is used.

An overlap removal procedure as described in ref. ⁸⁵ is applied to resolve the ambiguity if lepton signals in the calorimeter are also reconstructed as hadronic jets.

Systematic uncertainties. Several of the most important systematic uncertainties in the measurement of $R(\tau/\mu)$ merit a more detailed discussion, which is provided here.

Owing to differences in the hadronic environment around the lepton between the Z and $t\bar{t}$ final states and the coarse binning in p_T^μ and $|\eta|$, which may not be able to encapsulate the full shape information, small biases can exist in the data-driven μ_{prompt} template distributions. The size of such a possible bias is estimated from the full difference between $\mu_{\text{prompt}}|d_0^\mu|$ templates from Z and $t\bar{t}$ in

simulation. This uncertainty is split into two components corresponding to the tail, $|d_0^\mu| \gtrsim 0.05$ mm, and core, $|d_0^\mu| \lesssim 0.05$ mm, to prevent the data from constraining the uncertainty by using the full $|d_0^\mu|$ distribution.

The breakdown of uncertainties contributing to the μ_{had} background control region normalization in the e - μ (μ - μ) channels is as follows: 4% (4%) due to the size of the same-sign dataset; 8% (3%) due to the choice of Monte Carlo generators used; 1.0% (1.3%) due to the uncertainty in the subtraction of the other processes in the same-sign control region.

The uncertainties due to the choice of Monte Carlo event generator for the μ_{prompt} , $\mu_{\tau(\rightarrow\mu)}$ and μ_{had} processes are estimated by varying different components of the modelling in a factorized way. The following variations are considered targeting different sources of uncertainty:

- Initial- and final-state radiation: A14 eigen-tune variations⁴⁶ of the strong coupling (α_s)
- Missing higher-order QCD corrections: factorization and renormalization scales simultaneously varied up and down by a factor of two
- Resummation scale uncertainty: POWHEG h_{damp} parameter varied from 1.5 to 3 m_{top} (symmetrized)
- Parton shower and hadronization model: Herwig 7^{86,87}, H7UE tune^{87,88} (symmetrized)
- Higher-order correction to top p_T spectrum: not applying the NNLO top p_T reweighting⁵⁹ (symmetrized)

In the cases where only a single alternative is given, the uncertainty is taken to be the deviation from the nominal result and then symmetrized, as indicated above. The effects on μ_{prompt} and $\mu_{\tau(\rightarrow\mu)}$ (collectively referred to as ‘signal’) are treated as correlated and the effects on μ_{had} are treated separately. The parton shower and hadronization uncertainty is separated into four nuisance parameters: one each corresponding to low and middle probe muon p_T^μ bins used in the fit, and two corresponding to the high p_T^μ bin where the uncertainty is further separated into components related to normalization and shape differences.

Auxiliary material. Additional auxiliary figures can be found at <https://atlas.web.cern.ch/Atlas/GROUPS/PHYSICS/PAPERS/TOPO-2018-29/>.

Data availability

The experimental data that support the findings of this study are available in HEPData with the identifier <https://www.hepdata.net/record/100232>.

Code availability

The ATLAS software is available at the following link: <https://gitlab.cern.ch/atlas/athena>.

References

1. Frixione, S., Nason, P. & Ridolfi, G. A positive-weight next-to-leading-order Monte Carlo for heavy flavour hadroproduction. *J. High Energy Phys.* **09**, 126 (2007).
2. Nason, P. A New method for combining NLO QCD with shower Monte Carlo algorithms. *J. High Energy Phys.* **11**, 040 (2004).
3. Frixione, S., Nason, P. & Oleari, C. Matching NLO QCD computations with parton shower simulations: the POWHEG method. *J. High Energy Phys.* **11**, 070 (2007).
4. Alioli, S. et al. A general framework for implementing NLO calculations in shower Monte Carlo programs: the POWHEG BOX. *J. High Energy Phys.* **06**, 043 (2010).
5. Ball, R. D. et al. Parton distributions for the LHC run II. *J. High Energy Phys.* **04**, 040 (2015).
6. Sjöstrand, T. et al. An introduction to PYTHIA 8.2. *Comput. Phys. Commun.* **191**, 159–177 (2015).
7. ATLAS Collaboration ATLAS Pythia 8 Tunes to 7-TeV Data (CERN, 2014); <https://cds.cern.ch/record/1966419>
8. Ball, R. D. et al. Parton distributions with LHC data. *Nucl. Phys. B* **867**, 244–289 (2013).
9. ATLAS Collaboration Studies on Top-Quark Monte Carlo Modelling for Top2016 (CERN, 2016); <https://cds.cern.ch/record/2216168>
10. Lange, D. J. The 49 particle decay simulation package. *Nucl. Instrum. Methods A* **462**, 152–155 (2001).
11. Beneke, M. et al. Hadronic top-quark pair production with NNLL threshold resummation. *Nucl. Phys. B* **855**, 695–741 (2012).
12. Cacciari, M. et al. Top-pair production at hadron colliders with next-to-next-to-leading logarithmic soft-gluon resummation. *Phys. Lett. B* **710**, 612–622 (2012).
13. Bärnreuther, P., Czakon, M. & Mitov, A. Percent-level-precision physics at the LHC: next-to-next-to-leading order QCD corrections to $q\bar{q} \rightarrow t\bar{t} + X$. *Phys. Rev. Lett.* **109**, 132001 (2012).
14. Czakon, M. & Mitov, A. NNLO corrections to top-pair production at hadron colliders: the all-fermionic scattering channels. *J. High Energy Phys.* **12**, 054 (2012).

54. Czakon, M. & Mitov, A. NNLO corrections to top pair production at hadron colliders: the quark–gluon reaction. *J. High Energy Phys.* **01**, 080 (2013).
55. Czakon, M., Fiedler, P. & Mitov, A. Total top–quark pair-production cross section at hadron colliders through $\mathcal{O}(\alpha_s^3)$. *Phys. Rev. Lett.* **110**, 252004 (2013).
56. Czakon, M. & Mitov, A. Top++: a program for the calculation of the top-pair cross-section at hadron colliders. *Comput. Phys. Commun.* **185**, 2930–2938 (2014).
57. Aliev, M. et al. HATHOR: hadronic top and heavy quarks cross section calculator. *Comput. Phys. Commun.* **182**, 1034–1046 (2011).
58. Kant, P. et al. HATHOR for single top-quark production: updated predictions and uncertainty estimates for single top-quark production in hadronic collisions. *Comput. Phys. Commun.* **191**, 74–89 (2015).
59. Czakon, M. et al. Top-pair production at the LHC through NNLO QCD and NLO EW. *J. High Energy Phys.* **10**, 186 (2017).
60. Frixione, S. et al. Single-top hadroproduction in association with a W boson. *J. High Energy Phys.* **07**, 029 (2008).
61. Alwall, J. et al. The automated computation of tree-level and next-to-leading order differential cross sections, and their matching to parton shower simulations. *J. High Energy Phys.* **07**, 079 (2014).
62. Gleisberg, T. et al. Event generation with SHERPA 1.1. *J. High Energy Phys.* **02**, 007 (2009).
63. Bothmann, E. et al. Event generation with Sherpa 2.2. *SciPost Phys.* **7**, 034 (2019).
64. Gleisberg, T. & Höche, S. Comix, a new matrix element generator. *J. High Energy Phys.* **12**, 039 (2008).
65. Cascioli, F., Maierhofer, P. & Pozzorini, S. Scattering amplitudes with open loops. *Phys. Rev. Lett.* **108**, 111601 (2012).
66. Denner, A., Dittmaier, S. & Hofer, L. Collier: a fortran-based complex one-loop library in extended regularizations. *Comput. Phys. Commun.* **212**, 220–238 (2017).
67. Schumann, S. & Krauss, F. A parton shower algorithm based on Catani–Seymour dipole factorisation. *J. High Energy Phys.* **03**, 038 (2008).
68. Höche, S. et al. A critical appraisal of NLO + PS matching methods. *J. High Energy Phys.* **09**, 049 (2012).
69. Höche, S. et al. QCD matrix elements + parton showers: the NLO case. *J. High Energy Phys.* **04**, 027 (2013).
70. Catani, S. et al. QCD matrix elements + parton showers. *J. High Energy Phys.* **11**, 063 (2001).
71. Höche, S. et al. QCD matrix elements and truncated showers. *J. High Energy Phys.* **05**, 053 (2009).
72. ATLAS Collaboration ATLAS Simulation of Boson Plus Jets Processes in Run 2 (CERN, 2017); <https://cds.cern.ch/record/2261937>
73. ATLAS Collaboration Multi-Boson Simulation for 13-TeV ATLAS Analyses (CERN, 2017); <https://cds.cern.ch/record/2261933>
74. Anastasiou, C. et al. High precision QCD at hadron colliders: electroweak gauge boson rapidity distributions at NNLO. *Phys. Rev. D* **69**, 094008 (2004).
75. de Florian, D. et al. Handbook of LHC Higgs Cross Sections: 4. Deciphering the Nature of the Higgs Sector CERN-2017-002-M. Preprint at <https://arxiv.org/pdf/1610.07922.pdf> (2016).
76. ATLAS Collaboration Performance of the ATLAS track reconstruction algorithms in dense environments in LHC run 2. *Eur. Phys. J. C* **77**, 673 (2017).
77. ATLAS Collaboration Early Inner Detector Tracking Performance in the 2015 Data at $\sqrt{s} = 13$ TeV (CERN, 2015); <https://cds.cern.ch/record/2110140>
78. ATLAS Collaboration Electron and photon performance measurements with the ATLAS detector using the 2015–2017 LHC proton–proton collision data. *J. Instrum.* **14**, P12006 (2019).
79. ATLAS Collaboration Topological cell clustering in the ATLAS calorimeters and its performance in LHC run 1. *Eur. Phys. J. C* **77**, 490 (2017).
80. Cacciari, M., Salam, G. P. & Soyez, G. The anti- k_t jet clustering algorithm. *J. High Energy Phys.* **04**, 063 (2008).
81. ATLAS Collaboration Jet energy scale measurements and their systematic uncertainties in proton–proton collisions at $\sqrt{s} = 13$ TeV with the ATLAS detector. *Phys. Rev. D* **96**, 072002 (2017).
82. ATLAS Collaboration Performance of pile-up mitigation techniques for jets in pp collisions at $\sqrt{s} = 8$ TeV using the ATLAS detector. *Eur. Phys. J. C* **76**, 581 (2016).
83. ATLAS Collaboration Measurements of b -jet tagging efficiency with the ATLAS detector using $t\bar{t}$ events at $t\bar{t}$. *J. High Energy Phys.* **08**, 089 (2018).
84. ATLAS Collaboration ATLAS b -jet identification performance and efficiency measurement with $t\bar{t}$ events in pp collisions at $t\bar{t}$. *Eur. Phys. J. C* **79**, 970 (2019).
85. Aad, G. et al. Observation of the associated production of a top quark and a Z boson in pp collisions at $\sqrt{s} = 13$ TeV with the ATLAS detector. *J. High Energy Phys.* **07**, 124 (2020).
86. Bähr, M. et al. Herwig++ physics and manual. *Eur. Phys. J. C* **58**, 639–707 (2008).
87. Bellm, J. et al. Herwig 7.0/Herwig++ 3.0 release note. *Eur. Phys. J. C* **76**, 196 (2016).
88. Harland-Lang, L. et al. Parton distributions in the LHC era: MMHT 2014 PDFs. *Eur. Phys. J. C* **75**, 204 (2015).

Acknowledgements

We thank CERN for the very successful operation of the LHC, as well as the support staff from our institutions, without whom ATLAS could not be operated efficiently. We acknowledge the support of ANPCyT, Argentina; YerPhI, Armenia; ARC, Australia; BMWFW and FWF, Austria; ANAS, Azerbaijan; SSTC, Belarus; CNPq and FAPESP, Brazil; NSERC, NRC and CFI, Canada; CERN; ANID, Chile; CAS, MOST and NSFC, China; COLCIENCIAS, Colombia; MSMT CR, MPO CR and VSC CR, Czech Republic; DNR and DNSRC, Denmark; IN2P3-CNRS and CEA-DRF/IRFU, France; SRNSFG, Georgia; BMBF, HGF and MPG, Germany; GSRT, Greece; RGC and Hong Kong SAR, China; ISF and Benoziyo Center, Israel; INFN, Italy; MEXT and JSPS, Japan; CNRST, Morocco; NWO, Netherlands; RCN, Norway; MNiSW and NCN, Poland; FCT, Portugal; MNE/IFA, Romania; MES of Russia and NRC KI, Russia Federation; JINR; MESTD, Serbia; MSSR, Slovakia; ARRS and MIZŠ, Slovenia; DST/NRF, South Africa; MICINN, Spain; SRC and Wallenberg Foundation, Sweden; SERI, SNSF and cantons of Bern and Geneva, Switzerland; MOST, Taiwan; TAEK, Turkey; STFC, United Kingdom; DOE and NSF, United States. In addition, individual groups and members have received support from BCKDF, CANARIE, Compute Canada and CRC, Canada; ERC, ERDF, Horizon 2020, Marie Skłodowska-Curie Actions and COST, European Union; Investissements d'Avenir Labex, Investissements d'Avenir Idex and ANR, France; DFG and AvH Foundation, Germany; Herakleitos, Thales and Aristeia programmes co-financed by EU-ESF and the Greek NSRF, Greece; BSF-NSF and GIF, Israel; La Caixa Banking Foundation, CERCA Programme Generalitat de Catalunya and PROMETEO and GenT Programmes Generalitat Valenciana, Spain; Göran Gustafssons Stiftelse, Sweden; The Royal Society and Leverhulme Trust, United Kingdom. The crucial computing support from all WLCG partners is acknowledged gratefully, in particular from CERN, the ATLAS Tier-1 facilities at TRIUMF (Canada), NDGF (Denmark, Norway, Sweden), CC-IN2P3 (France), KIT/GridKA (Germany), INFN-CNAF (Italy), NL-T1 (Netherlands), PIC (Spain), ASGC (Taiwan), RAL (United Kingdom) and BNL (United States), the Tier-2 facilities worldwide and large non-WLCG resource providers. Major contributors of computing resources are listed at <https://cds.cern.ch/record/2717821>.

Author contributions

All authors have contributed to the publication, being variously involved in the design and the construction of the detectors, in writing software, calibrating subsystems, operating the detectors and acquiring data, and finally analysing the processed data. The ATLAS Collaboration members discussed and approved the scientific results. The manuscript was prepared by a subgroup of authors appointed by the collaboration and subject to an internal collaboration-wide review process. All authors reviewed and approved the final version of the manuscript.

Competing interests

The authors declare no competing interests.

Additional information

Correspondence and requests for materials should be addressed to G.A.

Peer review information *Nature Physics* thanks Thomas Kuhr and the other, anonymous, reviewer(s) for their contribution to the peer review of this work.

Reprints and permissions information is available at www.nature.com/reprints.

ATLAS Collaboration

G. Aad¹, B. Abbott², D. C. Abbott³, A. Abed Abud⁴, K. Abeling⁵, D. K. Abhayasinghe⁶, S. H. Abidi⁷, O. S. AbouZeid⁸, N. L. Abraham⁹, H. Abramowicz¹⁰, H. Abreu¹¹, Y. Abulaiti¹², B. S. Acharya^{13,14}, B. Achkar⁵, L. Adam¹⁵, C. Adam Bourdarios¹⁶, L. Adamczyk¹⁷, L. Adamek⁷, J. Adelman¹⁸, M. Adersberger¹⁹, A. Adiguzel²⁰, S. Adorni²¹, T. Adye²², A. A. Affolder²³, Y. Afik¹¹, C. Agapopoulou²⁴, M. N. Agaras²⁵, A. Aggarwal²⁶, C. Agheorghiesei²⁷, J. A. Aguilar-Saavedra^{28,29}, A. Ahmad⁴, F. Ahmadov³⁰, W. S. Ahmed³¹, X. Ai³², G. Aielli^{33,34}, S. Akatsuka³⁵, M. Akbiyik¹⁵, T. P. A. Åkesson³⁶, E. Akilli²¹, A. V. Akimov³⁷, K. Al Khoury²⁴, G. L. Alberghi^{38,39}, J. Albert⁴⁰, M. J. Alconada Verzini¹⁰, S. Alderweireldt⁴, M. Aleksa⁴, I. N. Aleksandrov³⁰, C. Alexa⁴¹, T. Alexopoulos⁴², A. Alfonsi⁴³, F. Alfonsi^{38,39}, M. Alhroob², B. Ali⁴⁴, S. Ali⁴⁵, M. Aliev⁴⁶, G. Alimonti⁴⁷, C. Allaire⁴, B. M. M. Allbrooke⁹, B. W. Allen⁴⁸, P. P. Allport⁴⁹, A. Aloisio^{50,51}, F. Alonso⁵², C. Alpigiani⁵³, E. Alunno Camelia^{33,34}, M. Alvarez Estevez⁵⁴, M. G. Alvigi^{50,51}, Y. Amaral Coutinho⁵⁵, A. Ambler³¹, L. Ambroz⁵⁶, C. Amelung⁵⁷, D. Amidei⁵⁸, S. P. Amor Dos Santos²⁸, S. Amoroso⁵⁹, C. S. Amrouche²¹, F. An⁶⁰, C. Anastopoulos⁶¹, N. Andari⁶², T. Andeen⁶³, J. K. Anders⁶⁴, S. Y. Andrean^{65,66}, A. Andreazza^{47,67}, V. Andrei⁶⁸, C. R. Anelli⁴⁰, S. Angelidakis⁶⁹, A. Angerami⁷⁰, A. V. Anisenkov^{71,72}, A. Annovi⁷³, C. Antel²¹, M. T. Anthony⁶¹, E. Antipov⁷⁴, M. Antonelli⁷⁵, D. J. A. Antrim⁷⁶, F. Anulli⁷⁷, M. Aoki⁷⁸, J. A. Aparisi Pozo⁷⁹, M. A. Aparo⁹, L. Aperio Bella⁵⁹, N. Aranzabal⁴, V. Araujo Ferraz⁸⁰, R. Araujo Pereira⁵⁵, C. Arcangeletti⁷⁵, A. T. H. Arce⁸¹, F. A. Arduh⁵², J.-F. Arguin⁸², S. Argyropoulos⁸³, J.-H. Arling⁵⁹, A. J. Armbruster⁴, A. Armstrong⁷⁶, O. Arnaez⁷, H. Arnold⁴³, Z. P. Arrubarrena Tame¹⁹, G. Artoni⁵⁶, H. Asada⁸⁴, K. Asai⁸⁵, S. Asai⁸⁶, T. Asawatavonvanich⁸⁷, N. Asbah⁸⁸, E. M. Asimakopoulou⁸⁹, L. Asquith⁹, J. Assahsah⁹⁰, K. Assamagan⁹¹, R. Astalos⁹², R. J. Atkin⁹³, M. Atkinson⁹⁴, N. B. Atlay⁹⁵, H. Atmani²⁴, K. Augsten⁴⁴, V. A. Austrup⁹⁶, G. Avolio⁴, M. K. Ayoub⁹⁷, G. Azuelos⁸², H. Bachacou⁶², K. Bachas⁹⁸, F. Backman^{65,66}, P. Bagnaia^{77,99}, M. Bahmani¹⁰⁰, H. Bahrasemani¹⁰¹, A. J. Bailey⁷⁹, V. R. Bailey⁹⁴, J. T. Baines²², C. Bakalis⁴², O. K. Baker¹⁰², P. J. Bakker⁴³, E. Bakos¹⁰³, D. Bakshi Gupta¹⁰⁴, S. Balaji¹⁰⁵, R. Balasubramanian⁴³, E. M. Baldin^{72,71}, P. Balek¹⁰⁶, F. Balli⁶², W. K. Balunas⁵⁶, J. Balz¹⁵, E. Banas¹⁰⁰, M. Bandieramonte¹⁰⁷, A. Bandyopadhyay¹⁰⁸, Sw. Banerjee¹⁰⁹, L. Barak¹⁰, W. M. Barbe²⁵, E. L. Barberio¹¹⁰, D. Barberis^{111,112}, M. Barbero¹, G. Barbour¹¹³, T. Barillari¹¹⁴, M.-S. Barisits⁴, J. Barkeloo⁴⁸, T. Barklow¹¹⁵, R. Barnea¹¹, B. M. Barnett²², R. M. Barnett³², Z. Barnovska-Blenessy¹¹⁶, A. Baroncelli¹¹⁶, G. Barone⁹¹, A. J. Barr⁵⁶, L. Barranco Navarro^{65,66}, F. Barreiro⁵⁴, J. Barreiro Guimarães da Costa⁹⁷, U. Barron¹⁰, S. Barsov¹¹⁷, F. Bartels⁶⁸, R. Bartoldus¹¹⁵, G. Bartolini¹, A. E. Barton¹¹⁸, P. Bartos⁹², A. Basalaev⁵⁹, A. Basan¹⁵, A. Bassalat²⁴, M. J. Basso⁷, R. L. Bates¹¹⁹, S. Batlamous¹²⁰, J. R. Batley¹²¹, B. Batool¹²², M. Battaglia²³, M. Bause^{77,99}, F. Bauer^{62,273}, P. Bauer¹⁰⁸, H. S. Bawa¹²³, A. Bayirli²⁰, J. B. Beacham⁸¹, T. Beau¹²⁴, P. H. Beauchemin¹²⁵, F. Becherer⁸³, P. Bechtle¹⁰⁸, H. C. Beck⁵, H. P. Beck^{64,239}, K. Becker¹²⁶, C. Becot⁵⁹, A. Beddall¹²⁷, A. J. Beddall¹²⁸, V. A. Bednyakov³⁰, M. Bedognetti⁴³, C. P. Bee¹²⁹, T. A. Beermann⁹⁶, M. Begalli⁵⁵, M. Begel⁹¹, A. Behera¹²⁹, J. K. Behr⁵⁹, F. Beisiegel¹⁰⁸, M. Belfkir¹⁶, A. S. Bell¹¹³, G. Bella¹⁰, L. Bellagamba³⁹, A. Bellerive¹³⁰, P. Bellos⁶⁹, K. Beloborodov^{72,71}, K. Belotskiy¹³¹, N. L. Belyaev¹³¹, D. Bencheikroun¹³², N. Benekos⁴², Y. Benhammou¹⁰, D. P. Benjamin¹², M. Benoit⁹¹, J. R. Bensinger⁵⁷, S. Bentvelsen⁴³, L. Beresford⁵⁶, M. Beretta⁷⁵, D. Berge⁹⁵, E. Bergeaas Kuutmann⁸⁹, N. Berger¹⁶, B. Bergmann⁴⁴, L. J. Bergsten⁵⁷, J. Beringer³², S. Berlendis¹³³, G. Bernardi¹²⁴, C. Bernius¹¹⁵, F. U. Bernlochner¹⁰⁸, T. Berry⁶, P. Berta¹⁵, A. Berthold¹³⁴, I. A. Bertram¹¹⁸, O. Bessidskaia Bylund⁹⁶, N. Besson⁶², A. Bethani¹³⁵, S. Bethke¹¹⁴, A. Betti¹³⁶, A. J. Bevan¹³⁷, J. Beyer¹¹⁴, D. S. Bhattacharya¹³⁸, P. Bhattarai⁵⁷, V. S. Bhopatkar¹², R. Bi¹⁰⁷, R. M. Bianchi¹⁰⁷, O. Biebel¹⁹, D. Biedermann⁹⁵, R. Bielski⁴,

K. Bierwagen¹⁵, N. V. Biesuz^{73,139}, M. Biglietti¹⁴⁰, T. R. V. Billoud⁴⁴, M. Bindi⁵, A. Bingul¹²⁷, C. Bini^{77,99}, S. Biondi^{39,38}, C. J. Birch-sykes¹³⁵, M. Birman¹⁰⁶, T. Bisanz⁴, J. P. Biswal¹⁴¹, D. Biswas¹⁰⁹, A. Bitadze¹³⁵, C. Bittrich¹³⁴, K. Bjørke¹⁴², T. Blazek⁹², I. Bloch⁵⁹, C. Blocker⁵⁷, A. Blue¹¹⁹, U. Blumenschein¹³⁷, G. J. Bobbink⁴³, V. S. Bobrovnikov^{72,71}, S. S. Bocchetta³⁶, D. Bogavac¹⁴³, A. G. Bogdanchikov^{72,71}, C. Bohm⁶⁵, V. Boisvert⁶, P. Bokan^{89,5}, T. Bold¹⁷, A. E. Bolz¹⁴⁴, M. Bomben¹²⁴, M. Bona¹³⁷, J. S. Bonilla⁴⁸, M. Boonekamp⁶², C. D. Booth⁶, A. G. Borbély¹¹⁹, H. M. Borecka-Bielska¹⁴⁵, L. S. Borgna¹¹³, A. Borisov¹⁴⁶, G. Borissov¹¹⁸, D. Bortoletto⁵⁶, D. Boscherini³⁹, M. Bosman¹⁴³, J. D. Bossio Sola³¹, K. Bouaouda¹³², J. Boudreau¹⁰⁷, E. V. Bouhova-Thacker¹¹⁸, D. Boumediene²⁵, A. Boveia¹⁴⁷, J. Boyd⁴, D. Boye¹⁴⁸, I. R. Boyko³⁰, A. J. Bozon⁶, J. Bracinik⁴⁹, N. Brahimi^{149,150}, G. Brandt⁹⁶, O. Brandt¹²¹, F. Braren⁵⁹, B. Brau³, J. E. Brau⁴⁸, W. D. Breaden Madden¹¹⁹, K. Brendlinger⁵⁹, R. Brenner¹¹, L. Brenner⁴, R. Brenner⁸⁹, S. Bressler¹⁰⁶, B. Brickwedde¹⁵, D. L. Briglin⁴⁹, D. Britton¹¹⁹, D. Britzger¹¹⁴, I. Brock¹⁰⁸, R. Brock¹⁵¹, G. Brooijmans⁷⁰, W. K. Brooks¹⁵², E. Brost⁹¹, P. A. Bruckman de Renstrom¹⁰⁰, B. Brüers⁵⁹, D. Bruncko¹⁵³, A. Bruni³⁹, G. Bruni³⁹, M. Bruschi³⁹, N. Bruscino^{77,99}, L. Bryngemark¹¹⁵, T. Buanes¹⁵⁴, Q. Buat¹²⁹, P. Buchholz¹²², A. G. Buckley¹¹⁹, I. A. Budagov³⁰, M. K. Bugge¹⁴², F. Bühner⁸³, O. Bulekov¹³¹, B. A. Bullard⁸⁸, T. J. Burch¹⁸, S. Burdin¹⁴⁵, C. D. Burgard⁴³, A. M. Burger⁷⁴, B. Burghgrave¹⁰⁴, J. T. P. Burr⁵⁹, C. D. Burton⁶³, J. C. Burzynski³, V. Büscher¹⁵, E. Buschmann⁵, P. J. Bussey¹¹⁹, J. M. Butler¹⁵⁵, C. M. Buttar¹¹⁹, J. M. Butterworth¹¹³, P. Butti⁴, W. Buttinger⁴, C. J. Buxo Vazquez¹⁵¹, A. Buzatu⁴⁵, A. R. Buzykaev^{72,71}, G. Cabras^{39,38}, S. Cabrera Urbán⁷⁹, D. Caforio¹⁵⁶, H. Cai¹⁰⁷, V. M. M. Cairo¹¹⁵, O. Cakir¹⁵⁷, N. Calace⁴, P. Calafiura³², G. Calderini¹²⁴, P. Calfayan¹⁵⁸, G. Callea¹¹⁹, L. P. Caloba⁵⁵, A. Caltabiano^{33,34}, S. Calvente Lopez⁵⁴, D. Calvet²⁵, S. Calvet²⁵, T. P. Calvet¹, M. Calvetti^{73,139}, R. Camacho Toro¹²⁴, S. Camarda⁴, D. Camarero Munoz⁵⁴, P. Camarri^{33,34}, M. T. Camerlingo^{140,159}, D. Cameron¹⁴², C. Camincher⁴, S. Campana⁴, M. Campanelli¹¹³, A. Camplani⁸, V. Canale^{50,51}, A. Canesse³¹, M. Cano Bret¹⁶⁰, J. Cantero⁷⁴, T. Cao¹⁰, Y. Cao⁹⁴, M. D. M. Capeans Garrido⁴, M. Capua^{161,162}, R. Cardarelli³³, F. Cardillo⁷⁹, G. Carducci^{161,162}, I. Carli¹⁶³, T. Carli⁴, G. Carlino⁵⁰, B. T. Carlson¹⁰⁷, E. M. Carlson^{40,164}, L. Carminati^{47,67}, R. M. D. Carney¹¹⁵, S. Caron²⁶, E. Carquin¹⁵², S. Carrá⁵⁹, G. Carratta^{39,38}, J. W. S. Carter⁷, T. M. Carter¹⁶⁵, M. P. Casado^{143,240}, A. F. Casha⁷, E. G. Castiglia¹⁰², F. L. Castillo⁷⁹, L. Castillo Garcia¹⁴³, V. Castillo Gimenez⁷⁹, N. F. Castro^{28,166}, A. Catinaccio⁴, J. R. Catmore¹⁴², A. Cattai⁴, V. Cavaliere⁹¹, V. Cavasinni^{73,139}, E. Celebi¹⁶⁷, F. Celli⁵⁶, K. Cerny¹⁶⁸, A. S. Cerqueira⁸⁰, A. Cerri⁹, L. Cerrito^{33,34}, F. Cerutti³², A. Cervelli^{39,38}, S. A. Cetin¹⁶⁷, Z. Chadi¹³², D. Chakraborty¹⁸, J. Chan¹⁰⁹, W. S. Chan⁴³, W. Y. Chan¹⁴⁵, J. D. Chapman¹²¹, B. Chargeishvili¹⁶⁹, D. G. Charlton⁴⁹, T. P. Charman¹³⁷, M. Chatterjee⁶⁴, C. C. Chau¹³⁰, S. Che¹⁴⁷, S. Chekanov¹², S. V. Chekulaev¹⁶⁴, G. A. Chelkov^{30,241}, B. Chen⁶⁰, C. Chen¹¹⁶, C. H. Chen⁶⁰, H. Chen¹⁷⁰, H. Chen⁹¹, J. Chen¹¹⁶, J. Chen⁷⁰, J. Chen⁵⁷, S. Chen¹⁷¹, S. J. Chen¹⁷⁰, X. Chen¹⁷², Y. Chen¹¹⁶, Y.-H. Chen⁵⁹, H. C. Cheng¹⁷³, H. J. Cheng⁹⁷, A. Cheplakov³⁰, E. Cheremushkina¹⁴⁶, R. Cherkaoui El Moursli¹²⁰, E. Cheu¹³³, K. Cheung¹⁷⁴, T. J. A. Chevaléras⁶², L. Chevalier⁶², V. Chiarella⁷⁵, G. Chiarelli⁷³, G. Chiodini¹⁷⁵, A. S. Chisholm⁴⁹, A. Chitan⁴¹, I. Chiu⁸⁶, Y. H. Chiu⁴⁰, M. V. Chizhov³⁰, K. Choi⁶³, A. R. Chomont^{77,99}, Y. S. Chow⁴³, L. D. Christopher¹⁷⁶, M. C. Chu¹⁷³, X. Chu^{97,177}, J. Chudoba¹⁷⁸, J. J. Chwastowski¹⁰⁰, L. Chytka¹⁶⁸, D. Cieri¹¹⁴, K. M. Ciesla¹⁰⁰, V. Cindro¹⁷⁹, I. A. Cioară⁴¹, A. Ciocio³², F. Cirotto^{50,51}, Z. H. Citron^{106,242}, M. Citterio⁴⁷, D. A. Ciubotaru⁴¹, B. M. Ciungu⁷, A. Clark²¹, M. R. Clark⁷⁰, P. J. Clark¹⁶⁵, S. E. Clawson¹³⁵, C. Clement^{65,66}, Y. Coadou¹, M. Cobal^{13,180}, A. Coccaro¹¹², J. Cochran⁶⁰, R. Coelho Lopes De Sa³, H. Cohen¹⁰, A. E. C. Coimbra⁴, B. Cole⁷⁰, A. P. Colijn⁴³, J. Collot¹⁸¹, P. Conde Muiño^{28,182}, S. H. Connell¹⁴⁸, I. A. Connelly¹¹⁹, S. Constantinescu⁴¹, F. Conventi^{50,243}, A. M. Cooper-Sarkar⁵⁶, F. Cormier¹⁸³, K. J. R. Cormier⁷, L. D. Corpe¹¹³, M. Corradi^{77,99}, E. E. Corrigan³⁶,

F. Corriveau^{31,244}, M. J. Costa⁷⁹, F. Costanza¹⁶, D. Costanzo⁶¹, G. Cowan⁶, J. W. Cowley¹²¹, J. Crane¹³⁵, K. Cranmer¹⁸⁴, R. A. Creager¹⁷¹, S. Crépe-Renaudin¹⁸¹, F. Crescioli¹²⁴, M. Cristinziani¹⁰⁸, V. Croft¹²⁵, G. Crosetti^{162,161}, A. Cueto¹⁶, T. Cuhadar Donszelmann⁷⁶, H. Cui^{97,177}, A. R. Cukierman¹¹⁵, W. R. Cunningham¹¹⁹, S. Czekierda¹⁰⁰, P. Czodrowski⁴, M. M. Czurylo¹⁴⁴, M. J. Da Cunha Sargedas De Sousa¹⁸⁵, J. V. Da Fonseca Pinto⁵⁵, C. Da Via¹³⁵, W. Dabrowski¹⁷, F. Dachs⁴, T. Dado¹⁸⁶, S. Dahbi¹⁷⁶, T. Dai⁵⁸, C. Dallapiccola³, M. Dam⁸, G. D'amen⁹¹, V. D'Amico^{140,159}, J. Damp¹⁵, J. R. Dandoy¹⁷¹, M. F. Daneri¹⁸⁷, M. Danninger¹⁰¹, V. Dao⁴, G. Darbo¹¹², O. Dartsis¹⁶, A. Dattagupta⁴⁸, T. Daubney⁵⁹, S. D'Auria^{47,67}, C. David¹⁸⁸, T. Davidek¹⁶³, D. R. Davis⁸¹, I. Dawson⁶¹, K. De¹⁰⁴, R. De Asmundis⁵⁰, M. De Beurs⁴³, S. De Castro^{39,38}, N. De Groot²⁶, P. de Jong⁴³, H. De la Torre¹⁵¹, A. De Maria¹⁷⁰, D. De Pedis⁷⁷, A. De Salvo⁷⁷, U. De Sanctis^{33,34}, M. De Santis^{33,34}, A. De Santo⁹, J. B. De Vivie De Regie²⁴, D. V. Dedovich³⁰, A. M. Deiana¹³⁶, J. Del Peso⁵⁴, Y. Delabat Diaz⁵⁹, D. Delgove²⁴, F. Deliot⁶², C. M. Delitzsch¹³³, M. Della Pietra^{50,51}, D. Della Volpe²¹, A. Dell'Acqua⁴, L. Dell'Asta^{33,34}, M. Delmastro¹⁶, C. Delporte²⁴, P. A. Delsart¹⁸¹, D. A. DeMarco⁷, S. Demers¹⁰², M. Demichev³⁰, G. Demontigny⁸², S. P. Denisov¹⁴⁶, L. D'Eramo¹⁸, D. Derendarz¹⁰⁰, J. E. Derkaoui⁹⁰, F. Derue¹²⁴, P. Dervan¹⁴⁵, K. Desch¹⁰⁸, K. Dette⁷, C. Deutsch¹⁰⁸, M. R. Devesa¹⁸⁷, P. O. Deviveiros⁴, F. A. Di Bello^{77,99}, A. Di Ciaccio^{33,34}, L. Di Ciaccio¹⁶, W. K. Di Clemente¹⁷¹, C. Di Donato^{50,51}, A. Di Girolamo⁴, G. Di Gregorio^{73,139}, B. Di Micco^{140,159}, R. Di Nardo^{140,159}, K. F. Di Petrillo⁸⁸, R. Di Sipio⁷, C. Diaconu¹, F. A. Dias⁴³, T. Dias Do Vale²⁸, M. A. Diaz¹⁸⁹, F. G. Diaz Capriles¹⁰⁸, J. Dickinson³², M. Didenko⁴⁶, E. B. Diehl⁵⁸, J. Dietrich⁹⁵, S. Díez Cornell⁵⁹, C. Díez Pardos¹²², A. Dimitrievska³², W. Ding¹⁷², J. Dingfelder¹⁰⁸, S. J. Dittmeier¹⁴⁴, F. Dittus⁴, F. Djama¹, T. Djobava¹⁶⁹, J. I. Djuvsland¹⁵⁴, M. A. B. Do Vale¹⁹⁰, M. Dobre⁴¹, D. Dodsworth⁵⁷, C. Doglioni³⁶, J. Dolejsi¹⁶³, Z. Dolezal¹⁶³, M. Donadelli¹⁹¹, B. Dong¹⁴⁹, J. Donini²⁵, A. D'onofrio¹⁷⁰, M. D'Onofrio¹⁴⁵, J. Dopke²², A. Doria⁵⁰, M. T. Dova⁵², A. T. Doyle¹¹⁹, E. Drechsler¹⁰¹, E. Dreyer¹⁰¹, T. Dreyer⁵, A. S. Drobac¹²⁵, D. Du¹⁸⁵, T. A. du Pree⁴³, Y. Duan¹⁵⁰, F. Dubinin³⁷, M. Dubovsky⁹², A. Dubreuil²¹, E. Duchovni¹⁰⁶, G. Duckeck¹⁹, O. A. Ducu^{4,41}, D. Duda¹¹⁴, A. Dudarev⁴, A. C. Dudder¹⁵, E. M. Duffield³², M. D'uffizi¹³⁵, L. Duflot²⁴, M. Dührssen⁴, C. Dülsen⁹⁶, M. Dumancic¹⁰⁶, A. E. Dumitriu⁴¹, M. Dunford⁶⁸, A. Duperrin¹, H. Duran Yildiz¹⁵⁷, M. Düren¹⁵⁶, A. Durglishvili¹⁶⁹, D. Duschinger¹³⁴, B. Dutta⁵⁹, D. Duvnjak¹⁹², G. I. Dyckes¹⁷¹, M. Dyndal⁴, S. Dysch¹³⁵, B. S. Dziedzic¹⁰⁰, M. G. Eggleston⁸¹, T. Eifert¹⁰⁴, G. Eigen¹⁵⁴, K. Einsweiler³², T. Ekelof⁸⁹, H. El Jarrari¹²⁰, V. Ellajosyula⁸⁹, M. Ellert⁸⁹, F. Ellinghaus⁹⁶, A. A. Elliot¹³⁷, N. Ellis⁴, J. Elmsheuser⁹¹, M. Elsing⁴, D. Emelianov²², A. Emerman⁷⁰, Y. Enari⁸⁶, M. B. Epland⁸¹, J. Erdmann¹⁸⁶, A. Ereditato⁶⁴, P. A. Erland¹⁰⁰, M. Errenst⁹⁶, M. Escalier²⁴, C. Escobar⁷⁹, O. Estrada Pastor⁷⁹, E. Etzion¹⁰, G. Evans^{28,193}, H. Evans¹⁵⁸, M. O. Evans⁹, A. Ezhilov¹¹⁷, F. Fabbri¹¹⁹, L. Fabbri^{39,38}, V. Fabiani¹²⁶, G. Facini¹²⁶, R. M. Fakhruddinov¹⁴⁶, S. Falciano⁷⁷, P. J. Falke¹⁰⁸, S. Falke⁴, J. Faltova¹⁶³, Y. Fang⁹⁷, Y. Fang⁹⁷, G. Fanourakis¹⁹⁴, M. Fanti^{47,67}, M. Faraj^{13,180}, A. Farbin¹⁰⁴, A. Farilla¹⁴⁰, E. M. Farina^{195,196}, T. Farooque¹⁵¹, S. M. Farrington¹⁶⁵, P. Farthouat⁴, F. Fassi¹²⁰, P. Fassnacht⁴, D. Fassouliotis⁶⁹, M. Fauci Giannelli¹⁶⁵, W. J. Fawcett¹²¹, L. Fayard²⁴, O. L. Fedin^{117,245}, W. Fedorko¹⁸³, A. Fehr⁶⁴, M. Feickert⁹⁴, L. Feligioni¹, A. Fell⁶¹, C. Feng¹⁸⁵, M. Feng⁸¹, M. J. Fenton⁷⁶, A. B. Fenyuk¹⁴⁶, S. W. Ferguson¹⁹⁷, J. Ferrando⁵⁹, A. Ferrante⁹⁴, A. Ferrari⁸⁹, P. Ferrari⁴³, R. Ferrari¹⁹⁵, D. E. Ferreira de Lima¹⁴⁴, A. Ferrer⁷⁹, D. Ferrere²¹, C. Ferretti⁵⁸, F. Fiedler¹⁵, A. Filipčić¹⁷⁹, F. Filthaut²⁶, K. D. Finelli¹⁵⁵, M. C. N. Fiolhais^{28,198,246}, L. Fiorini⁷⁹, F. Fischer¹⁹, J. Fischer¹⁵, W. C. Fisher¹⁵¹, T. Fitschen⁴⁹, I. Fleck¹²², P. Fleischmann⁵⁸, T. Flick⁹⁶, B. M. Flierl¹⁹, L. Flores¹⁷¹, L. R. Flores Castillo¹⁷³, F. M. Follega^{199,200}, N. Fomin¹⁵⁴, J. H. Foo⁷, G. T. Forcolin^{199,200}, B. C. Forland¹⁵⁸, A. Formica⁶², F. A. Förster¹⁴³, A. C. Forti¹³⁵, E. Fortin¹, M. G. Foti⁵⁶, D. Fournier²⁴, H. Fox¹¹⁸, P. Francavilla^{73,139},

S. Francescato^{77,99}, M. Franchini^{39,38}, S. Franchino⁶⁸, D. Francis⁴, L. Franco¹⁶, L. Franconi⁶⁴, M. Franklin⁸⁸, G. Frattari^{77,99}, A. N. Fray¹³⁷, P. M. Freeman⁴⁹, B. Freund⁸², W. S. Freund⁵⁵, E. M. Freundlich¹⁸⁶, D. C. Frizzell², D. Froidevaux⁴, J. A. Frost⁵⁶, M. Fujimoto⁸⁵, C. Fukunaga²⁰¹, E. Fullana Torregrosa⁷⁹, T. Fusayasu²⁰², J. Fuster⁷⁹, A. Gabrielli^{39,38}, A. Gabrielli⁴, S. Gadatsch²¹, P. Gadow¹¹⁴, G. Gagliardi^{112,111}, L. G. Gagnon⁸², G. E. Gallardo⁵⁶, E. J. Gallas⁵⁶, B. J. Gallop²², R. Gamboa Goni¹³⁷, K. K. Gan¹⁴⁷, S. Ganguly¹⁰⁶, J. Gao¹¹⁶, Y. Gao¹⁶⁵, Y. S. Gao^{123,247}, F. M. Garay Walls¹⁸⁹, C. García⁷⁹, J. E. García Navarro⁷⁹, J. A. García Pascual⁹⁷, C. Garcia-Argos⁸³, M. Garcia-Sciveres³², R. W. Gardner²⁰³, N. Garelli¹¹⁵, S. Gargiulo⁸³, C. A. Garner⁷, V. Garonne¹⁴², S. J. Gasiorowski⁵³, P. Gaspar⁵⁵, A. Gaudiello^{112,111}, G. Gaudio¹⁹⁵, P. Gauzzi^{77,99}, I. L. Gavrilenko³⁷, A. Gavrilyuk²⁰⁴, C. Gay¹⁸³, G. Gaycken⁵⁹, E. N. Gazis⁴², A. A. Geanta⁴¹, C. M. Gee²³, C. N. P. Gee²², J. Geisen³⁶, M. Geisen¹⁵, C. Gemme¹¹², M. H. Genest¹⁸¹, C. Geng⁵⁸, S. Gentile^{77,99}, S. George⁶, T. Geralis¹⁹⁴, L. O. Gerlach⁵, P. Gessinger-Befurt¹⁵, G. Gessner¹⁸⁶, S. Ghasemi¹²², M. Ghasemi Bostanabad⁴⁰, M. Ghneimat¹²², A. Ghosh²⁴, A. Ghosh¹⁶⁰, B. Giacobbe³⁹, S. Giagu^{77,99}, N. Giangiacomi^{39,38}, P. Giannetti⁷³, A. Giannini^{50,51}, G. Giannini¹⁴³, S. M. Gibson⁶, M. Gignac²³, D. T. Gil²⁰⁵, B. J. Gilbert⁷⁰, D. Gillberg¹³⁰, G. Gilles⁹⁶, N. E. K. Gillwald⁵⁹, D. M. Gingrich¹⁴¹, M. P. Giordani^{13,180}, P. F. Giraud⁶², G. Giugliarelli^{13,180}, D. Giugni¹⁴⁷, F. Giuli^{33,34}, S. Gkaitatzis⁹⁸, I. Gkialas^{69,248}, E. L. Gkougkousis¹⁴³, P. Gkoutoumis⁴², L. K. Gladilin²⁰⁶, C. Glasman⁵⁴, J. Glatzer¹⁴³, P. C. F. Glaysheer⁵⁹, A. Glazov⁵⁹, G. R. Gledhill⁴⁸, I. Gnesi^{162,249}, M. Goblirsch-Kolb⁵⁷, D. Godin⁸², S. Goldfarb¹¹⁰, T. Golling²¹, D. Golubkov¹⁴⁶, A. Gomes^{28,193}, R. Goncalves Gama⁵, R. Gonçalo^{28,198}, G. Gonella⁴⁸, L. Gonella⁴⁹, A. Gongadze³⁰, F. Gonnella⁴⁹, J. L. Gonski⁷⁰, S. González de la Hoz⁷⁹, S. Gonzalez Fernandez¹⁴³, R. Gonzalez Lopez¹⁴⁵, C. Gonzalez Renteria³², R. Gonzalez Suarez⁸⁹, S. Gonzalez-Sevilla²¹, G. R. Gonzalvo Rodriguez⁷⁹, L. Goossens⁴, N. A. Gorasia⁴⁹, P. A. Gorbounov²⁰⁴, H. A. Gordon⁹¹, B. Gorini⁴, E. Gorini^{175,207}, A. Gorišek¹⁷⁹, A. T. Goshaw⁸¹, M. I. Gostkin³⁰, C. A. Gottardo²⁶, M. Goughri²⁰⁸, A. G. Goussiou⁵³, N. Govender¹⁴⁸, C. Goy¹⁶, I. Grabowska-Bold¹⁷, E. C. Graham¹⁴⁵, J. Gramling⁷⁶, E. Gramstad¹⁴², S. Grancagnolo⁹⁵, M. Grandi⁹, V. Gratchev¹¹⁷, P. M. Gravila²⁰⁹, F. G. Gravili^{175,207}, C. Gray¹¹⁹, H. M. Gray³², C. Greife¹⁰⁸, K. Gregersen³⁶, I. M. Gregor⁵⁹, P. Grenier¹¹⁵, K. Grevtsov⁵⁹, C. Grieco¹⁴³, N. A. Grieser², A. A. Grillo²³, K. Grimm^{123,250}, S. Grinstein^{143,251}, J.-F. Grivaz²⁴, S. Groh¹⁵, E. Gross¹⁰⁶, J. Grosse-Knetter⁵, Z. J. Grout¹¹³, C. Grud⁵⁸, A. Grummer²¹⁰, J. C. Grundy⁵⁶, L. Guan⁵⁸, W. Guan¹⁰⁹, C. Gubbels¹⁸³, J. Guenther²¹¹, A. Guerguichon²⁴, J. G. R. Guerrero Rojas⁷⁹, F. Guescini¹¹⁴, D. Guest⁷⁶, R. Gugel¹⁵, A. Guida⁵⁹, T. Guillemin¹⁶, S. Guindon⁴, J. Guo¹⁴⁹, W. Guo⁵⁸, Y. Guo¹¹⁶, Z. Guo¹, R. Gupta⁵⁹, S. Gurbuz²⁰, G. Gustavino², M. Guth⁸³, P. Gutierrez², C. Gutsche¹¹³, C. Guyot⁶², C. Gwenlan⁵⁶, C. B. Gwilliam¹⁴⁵, E. S. Haaland¹⁴², A. Haas¹⁸⁴, C. Haber³², H. K. Hadavand¹⁰⁴, A. Hadei¹¹⁶, M. Haleem¹³⁸, J. Haley⁷⁴, J. J. Hall⁶¹, G. Halladjian¹⁵¹, G. D. Hallowell¹, K. Hamano⁴⁰, H. Hamdaoui¹²⁰, M. Hamer¹⁰⁸, G. N. Hamity¹⁶⁵, K. Han^{116,24}, L. Han¹⁷⁰, L. Han¹¹⁶, S. Han³², Y. F. Han⁷, K. Hanagaki^{78,252}, M. Hance²³, D. M. Handl¹⁹, M. D. Hank²⁰³, R. Hankache¹²⁴, E. Hansen³⁶, J. B. Hansen⁸, J. D. Hansen⁸, M. C. Hansen¹⁰⁸, P. H. Hansen⁸, E. C. Hanson¹³⁵, K. Hara²¹², T. Harenberg⁹⁶, S. Harkusha²¹³, P. F. Harrison¹²⁶, N. M. Hartman¹¹⁵, N. M. Hartmann¹⁹, Y. Hasegawa²¹⁴, A. Hasib¹⁶⁵, S. Hassani⁶², S. Haug⁶⁴, R. Hauser¹⁵¹, L. B. Havener⁷⁰, M. Havranek⁴⁴, C. M. Hawkes⁴⁹, R. J. Hawkings⁴, S. Hayashida⁸⁴, D. Hayden¹⁵¹, C. Hayes⁵⁸, R. L. Hayes¹⁸³, C. P. Hays⁵⁶, J. M. Hays¹³⁷, H. S. Hayward¹⁴⁵, S. J. Haywood²², F. He¹¹⁶, Y. He⁸⁷, M. P. Heath¹⁶⁵, V. Hedberg³⁶, A. L. Heggelund¹⁴², C. Heidegger⁸³, K. K. Heidegger⁸³, W. D. Heidorn⁶⁰, J. Heilman¹³⁰, S. Heim⁵⁹, T. Heim³², B. Heinemann^{59,253}, J. G. Heinlein¹⁷¹, J. J. Heinrich⁴⁸, L. Heinrich⁴, J. Hejbal¹⁷⁸, L. Helary⁵⁹, A. Held¹⁸⁴, S. Hellesund¹⁴², C. M. Helling²³, S. Hellman^{65,66}, C. Helsen⁴, R. C. W. Henderson¹¹⁸, Y. Heng¹⁰⁹, L. Henkelmann¹²¹, A. M. Henriques Correia⁴, H. Herde⁵⁷, Y. Hernández Jiménez¹⁷⁶, H. Herr¹⁵, M. G. Herrmann¹⁹,

T. Herrmann¹³⁴, G. Herten⁸³, R. Hertenberger¹⁹, L. Hervas⁴, T. C. Herwig¹⁷¹, G. G. Hesketh¹¹³, N. P. Hessey¹⁶⁴, H. Hibi²¹⁵, S. Higashino⁷⁸, E. Higón-Rodríguez⁷⁹, K. Hildebrand²⁰³, J. C. Hill¹²¹, K. K. Hill⁹¹, K. H. Hiller⁵⁹, S. J. Hillier⁴⁹, M. Hils¹³⁴, I. Hinchliffe³², F. Hinterkeuser¹⁰⁸, M. Hirose²¹⁶, S. Hirose²¹², D. Hirschbuehl⁹⁶, B. Hiti¹⁷⁹, O. Hladik¹⁷⁸, J. Hobbs¹²⁹, N. Hod¹⁰⁶, M. C. Hodgkinson⁶¹, A. Hoecker⁴, D. Hohn⁸³, D. Hohov²⁴, T. Holm¹⁰⁸, T. R. Holmes²⁰³, M. Holzbock¹¹⁴, L. B. A. H. Hommels¹²¹, T. M. Hong¹⁰⁷, J. C. Honig⁸³, A. Hönle¹¹⁴, B. H. Hooberman⁹⁴, W. H. Hopkins¹², Y. Horii⁸⁴, P. Horn¹³⁴, L. A. Horyn²⁰³, S. Hou⁴⁵, A. Hoummada¹³², J. Howarth¹¹⁹, J. Hoya⁵², M. Hrabovsky¹⁶⁸, J. Hrivnac²⁴, A. Hrynevich²¹⁷, T. Hryn'ova¹⁶, P. J. Hsu¹⁷⁴, S.-C. Hsu⁵³, Q. Hu⁹¹, S. Hu¹⁴⁹, Y. F. Hu^{97,177,254}, D. P. Huang¹¹³, X. Huang¹⁷⁰, Y. Huang¹¹⁶, Y. Huang⁹⁷, Z. Hubacek⁴⁴, F. Hubaut¹, M. Huebner¹⁰⁸, F. Huegging¹⁰⁸, T. B. Huffman⁵⁶, M. Huhtinen⁴, R. Hulsken¹⁸¹, R. F. H. Hunter¹³⁰, N. Huseynov^{30,255}, J. Huston¹⁵¹, J. Huth⁸⁸, R. Hyneman¹¹⁵, S. Hyrych⁹², G. Iacobucci²¹, G. Iakovidis⁹¹, I. Ibragimov¹²², L. Iconomidou-Fayard²⁴, P. Iengo⁴, R. Ignazzi⁸, O. Igonkina^{43,256,273}, R. Iguchi⁸⁶, T. Iizawa²¹, Y. Ikegami⁷⁸, M. Ikeno⁷⁸, N. Ilic^{26,7,244}, F. Iltzsche¹³⁴, H. Imam¹³², G. Introzzi^{195,196}, M. Iodice¹⁴⁰, K. Iordanidou¹⁶⁴, V. Ippolito^{77,99}, M. F. Isacson⁸⁹, M. Ishino⁸⁶, W. Islam⁷⁴, C. Issever^{95,59}, S. Istin¹¹, J. M. Iturbe Ponce¹⁷³, R. Iuppa^{199,200}, A. Ivina¹⁰⁶, J. M. Izen¹⁹⁷, V. Izzo⁵⁰, P. Jacka¹⁷⁸, P. Jackson¹⁹², R. M. Jacobs⁵⁹, B. P. Jaeger¹⁰¹, V. Jain²¹⁸, G. Jäkel⁹⁶, K. B. Jakobi¹⁵, K. Jakobs⁸³, T. Jakoubek¹⁰⁶, J. Jamieson¹¹⁹, K. W. Janas¹⁷, R. Jansky²¹, M. Janus⁵, P. A. Janus¹⁷, G. Jarlskog³⁶, A. E. Jaspan¹⁴⁵, N. Javadov^{30,255}, T. Javůrek⁴, M. Javurkova³, F. Jeanneau⁶², L. Jeanty⁴⁸, J. Jejelava²¹⁹, P. Jenni^{83,257}, N. Jeong⁵⁹, S. Jézéquel¹⁶, H. Ji¹⁰⁹, J. Jia¹²⁹, Z. Jia¹⁷⁰, H. Jiang⁶⁰, Y. Jiang¹¹⁶, Z. Jiang¹¹⁵, S. Jiggins⁸³, F. A. Jimenez Morales²⁵, J. Jimenez Pena¹¹⁴, S. Jin¹⁷⁰, A. Jinaru⁴¹, O. Jinnouchi⁸⁷, H. Jivan¹⁷⁶, P. Johansson⁶¹, K. A. Johns¹³³, C. A. Johnson¹⁵⁸, E. Jones¹²⁶, R. W. L. Jones¹¹⁸, S. D. Jones⁹, T. J. Jones¹⁴⁵, J. Jongmanns⁶⁸, J. Jovicevic⁴, X. Ju³², J. J. Junggeburth¹¹⁴, A. Juste Rozas^{143,251}, A. Kaczmarska¹⁰⁰, M. Kado^{77,99}, H. Kagan¹⁴⁷, M. Kagan¹¹⁵, A. Kahn⁷⁰, C. Kahra¹⁵, T. Kaji²²⁰, E. Kajomovitz¹¹, C. W. Kalderon⁹¹, A. Kaluza¹⁵, A. Kamenshchikov¹⁴⁶, M. Kaneda⁸⁶, N. J. Kang²³, S. Kang⁶⁰, Y. Kano⁸⁴, J. Kanzaki⁷⁸, L. S. Kaplan¹⁰⁹, D. Kar¹⁷⁶, K. Karava⁵⁶, M. J. Kareem¹⁸⁸, I. Karkanas⁹⁸, S. N. Karpov³⁰, Z. M. Karpova³⁰, V. Kartvelishvili¹¹⁸, A. N. Karyukhin¹⁴⁶, E. Kasimi⁹⁸, A. Kastanas^{65,66}, C. Kato¹⁵⁰, J. Katzy⁵⁹, K. Kawade²¹⁴, K. Kawagoe²²¹, T. Kawaguchi⁸⁴, T. Kawamoto⁶², G. Kawamura⁵, E. F. Kay⁴⁰, S. Kazakos¹⁴³, V. F. Kazanin^{72,71}, J. M. Keaveney⁹³, R. Keeler⁴⁰, J. S. Keller¹³⁰, E. Kellermann³⁶, D. Kelsey⁹, J. J. Kempster⁴⁹, J. Kendrick⁴⁹, K. E. Kennedy⁷⁰, O. Kepka¹⁷⁸, S. Kersten⁹⁶, B. P. Kerševan¹⁷⁹, S. Ketabchi Haghighat⁷, M. Khader⁹⁴, F. Khalil-Zada²²², M. Khandoga⁶², A. Khanov⁷⁴, A. G. Kharlamov^{72,71}, T. Kharlamova^{72,71}, E. E. Khoda¹⁸³, A. Khodinov⁴⁶, T. J. Khoo²¹¹, G. Khoriali¹³⁸, E. Khramov³⁰, J. Khubua¹⁶⁹, S. Kido²¹⁵, M. Kiehn⁴, E. Kim⁸⁷, Y. K. Kim²⁰³, N. Kimura¹¹³, A. Kirchhoff⁵, D. Kirchmeier¹³⁴, J. Kirk²², A. E. Kiryunin¹¹⁴, T. Kishimoto⁸⁶, D. P. Kisliuk⁷, V. Kitali⁵⁹, C. Kitsaki⁴², O. Kivernyk¹⁰⁸, T. Klapdor-Kleingrothaus⁸³, M. Klassen⁶⁸, C. Klein¹³⁰, M. H. Klein⁵⁸, M. Klein¹⁴⁵, U. Klein¹⁴⁵, K. Kleinknecht¹⁵, P. Klimek⁴, A. Klimentov⁹¹, T. Klingl¹⁰⁸, T. Klioutchnikova⁴, F. F. Klitzner¹⁹, P. Kluit⁴³, S. Kluth¹¹⁴, E. Kneringer²¹¹, E. B. F. G. Knoop¹, A. Knue⁸³, D. Kobayashi²²¹, M. Kobel¹³⁴, M. Kocian¹¹⁵, T. Kodama⁸⁶, P. Kodys¹⁶³, D. M. Koeck⁹, P. T. Koenig¹⁰⁸, T. Koffas¹³⁰, N. M. Köhler⁴, M. Kolb⁶², I. Koletsou¹⁶, T. Komarek¹⁶⁸, T. Kondo⁷⁸, K. Köneke⁸³, A. X. Y. Kong¹⁹², A. C. König²⁶, T. Kono⁸⁵, V. Konstantinides¹¹³, N. Konstantinidis¹¹³, B. Konya³⁶, R. Kopeliansky¹⁵⁸, S. Koperny¹⁷, K. Korcyl¹⁰⁰, K. Kordas⁹⁸, G. Koren¹⁰, A. Korn¹¹³, I. Korolkov¹⁴³, E. V. Korolkova⁶¹, N. Korotkova²⁰⁶, O. Kortner¹¹⁴, S. Kortner¹¹⁴, V. V. Kostyukhin^{61,46}, A. Kotskechagia²⁴, A. Kotwal⁸¹, A. Koulouris⁴², A. Kourkoulis-Charalampidi^{195,196}, C. Kourkoulis⁶⁹, E. Kourlitis¹², V. Kouskoura⁹¹, R. Kowalewski⁴⁰, W. Kozanecki¹³⁵, A. S. Kozhin¹⁴⁶, V. A. Kramarenko²⁰⁶, G. Kramberger¹⁷⁹, D. Krasnopevtsev¹¹⁶, M. W. Krasny¹²⁴, A. Krasznahorkay⁴, D. Krauss¹¹⁴, J. A. Kremer¹⁵, J. Kretzschmar¹⁴⁵, P. Krieger⁷,

F. Krieter¹⁹, A. Krishnan¹⁴⁴, M. Krivos¹⁶³, K. Krizka³², K. Kroeninger¹⁸⁶, H. Kroha¹¹⁴, J. Kroll¹⁷⁸, J. Kroll¹⁷¹, K. S. Krowpman¹⁵¹, U. Kruchonak³⁰, H. Krüger¹⁰⁸, N. Krumnack⁶⁰, M. C. Kruse⁸¹, J. A. Krzysiak¹⁰⁰, A. Kubota⁸⁷, O. Kuchinskaia⁴⁶, S. Kuday²²³, D. Kuechler⁵⁹, J. T. Kuechler⁵⁹, S. Kuehn⁴, T. Kuhl⁵⁹, V. Kukhtin³⁰, Y. Kulchitsky^{213,258}, S. Kuleshov²²⁴, Y. P. Kulinich⁹⁴, M. Kuna¹⁸¹, A. Kupco¹⁷⁸, T. Kupfer¹⁸⁶, O. Kuprash⁸³, H. Kurashige²¹⁵, L. L. Kurchaninov¹⁶⁴, Y. A. Kurochkin²¹³, A. Kurova¹³¹, M. G. Kurth^{97,177}, E. S. Kuwertz⁴, M. Kuze⁸⁷, A. K. Kvam⁵³, J. Kvita¹⁶⁸, T. Kwan³¹, F. La Ruffa^{162,161}, C. Lacasta⁷⁹, F. Lacava^{77,99}, D. P. J. Lack¹³⁵, H. Lacker⁹⁵, D. Lacour¹²⁴, E. Ladygin³⁰, R. Lafaye¹⁶, B. Laforge¹²⁴, T. Lagouri²²⁵, S. Lai⁵, I. K. Lakomic¹⁷, J. E. Lambert², S. Lammers¹⁵⁸, W. Lampl¹³³, C. Lampoudis⁹⁸, E. Lançon⁹¹, U. Landgraf⁸³, M. P. J. Landon¹³⁷, V. S. Lang⁸³, J. C. Lange⁵, R. J. Langenberg³, A. J. Lankford⁷⁶, F. Lanni⁹¹, K. Lantzscht¹⁰⁸, A. Lanza¹⁹⁵, A. Lapertosa^{112,111}, J. F. Laporte⁶², T. Lari⁴⁷, F. Lasagni Manghi^{39,38}, M. Lassnig⁴, V. Latonova¹⁷⁸, T. S. Lau¹⁷³, A. Laudrain¹⁵, A. Laurier¹³⁰, M. Lavorgna^{50,51}, S. D. Lawlor⁶, M. Lazzaroni^{47,67}, B. Le¹³⁵, E. Le Guirriec¹, A. Lebedev⁶⁰, M. LeBlanc¹³³, T. LeCompte¹², F. Ledroit-Guillon¹⁸¹, A. C. A. Lee¹¹³, C. A. Lee⁹¹, G. R. Lee¹⁵⁴, L. Lee⁸⁸, S. C. Lee⁴⁵, S. Lee⁶⁰, B. Lefebvre¹⁶⁴, H. P. Lefebvre⁶, M. Lefebvre⁴⁰, C. Leggett³², K. Lehmann¹⁰¹, N. Lehmann⁶⁴, G. Lehmann Miotto⁴, W. A. Leight⁵⁹, A. Leisos^{98,259}, M. A. L. Leite¹⁹¹, C. E. Leitgeb¹⁹, R. Leitner¹⁶³, D. Lellouch^{106,273}, K. J. C. Leney¹³⁶, T. Lenz¹⁰⁸, S. Leone⁷³, C. Leonidopoulos¹⁶⁵, A. Leopold¹²⁴, C. Leroy⁸², R. Les¹⁵¹, C. G. Lester¹²¹, M. Levchenko¹¹⁷, J. Levêque¹⁶, D. Levin⁵⁸, L. J. Levinson¹⁰⁶, D. J. Lewis⁴⁹, B. Li¹⁷², B. Li⁵⁸, C.-Q. Li^{149,150}, F. Li¹⁴⁹, H. Li¹¹⁶, H. Li¹⁸⁵, J. Li¹⁴⁹, K. Li⁵³, L. Li¹⁴⁹, M. Li^{97,177}, Q. Li^{97,177}, Q. Y. Li¹¹⁶, S. Li^{150,149}, X. Li⁵⁹, Y. Li⁵⁹, Z. Li¹⁸⁵, Z. Li⁵⁶, Z. Li³¹, Z. Liang⁹⁷, M. Liberatore⁵⁹, B. Liberti³³, K. Lie²²⁶, S. Lim⁹¹, C. Y. Lin¹²¹, K. Lin¹⁵¹, R. A. Linck¹⁵⁸, R. E. Lindley¹³³, J. H. Lindon⁴⁹, A. Linss⁵⁹, A. L. Lioni²¹, E. Lipeles¹⁷¹, A. Lipniacka¹⁵⁴, T. M. Liss^{94,260}, A. Lister¹⁸³, J. D. Little¹⁰⁴, B. Liu⁶⁰, B. X. Liu¹⁰¹, H. B. Liu⁹¹, J. B. Liu¹¹⁶, J. K. K. Liu²⁰³, K. Liu^{150,149}, M. Liu¹¹⁶, M. Y. Liu¹¹⁶, P. Liu⁹⁷, X. Liu¹¹⁶, Y. Liu⁵⁹, Y. Liu^{97,177}, Y. L. Liu⁵⁸, Y. W. Liu¹¹⁶, M. Livan^{195,196}, A. Lleres¹⁸¹, J. Llorente Merino¹⁰¹, S. L. Lloyd¹³⁷, C. Y. Lo²²⁷, E. M. Lobodzinska⁵⁹, P. Loch¹³³, S. Loffredo^{33,34}, T. Lohse⁹⁵, K. Lohwasser⁶¹, M. Lokajicek¹⁷⁸, J. D. Long⁹⁴, R. E. Long¹¹⁸, I. Longarini^{77,99}, L. Longo⁴, K. A. Looper¹⁴⁷, I. Lopez Paz¹³⁵, A. Lopez Solis⁶¹, J. Lorenz¹⁹, N. Lorenzo Martinez¹⁶, A. M. Lory¹⁹, P. J. Lösel¹⁹, A. Lösle⁸³, X. Lou^{65,66}, X. Lou⁹⁷, A. Lounis²⁴, J. Love¹², P. A. Love¹¹⁸, J. J. Lozano Bahilo⁷⁹, M. Lu¹¹⁶, Y. J. Lu¹⁷⁴, H. J. Lubatti⁵³, C. Luci^{77,99}, F. L. Lucio Alves¹⁷⁰, A. Lucotte¹⁸¹, F. Luehring¹⁵⁸, I. Luise¹²⁹, L. Luminari⁷⁷, B. Lund-Jensen²²⁸, M. S. Lutz¹⁰, D. Lynn⁹¹, H. Lyons¹⁴⁵, R. Lysak¹⁷⁸, E. Lytken³⁶, F. Lyu⁹⁷, V. Lyubushkin³⁰, T. Lyubushkina³⁰, H. Ma⁹¹, L. L. Ma¹⁸⁵, Y. Ma¹¹³, D. M. Mac Donell⁴⁰, G. Maccarrone⁷⁵, A. Macchiolo¹¹⁴, C. M. Macdonald⁶¹, J. C. MacDonald⁶¹, J. Machado Miguens¹⁷¹, D. Madaffari⁷⁹, R. Madar²⁵, W. F. Mader¹³⁴, M. Madugoda Ralalage Don⁷⁴, N. Madysa¹³⁴, J. Maeda²¹⁵, T. Maeno⁹¹, M. Maerker¹³⁴, V. Magerl⁸³, N. Magini⁶⁰, J. Magro^{13,180,261}, D. J. Mahon⁷⁰, C. Maidantchik⁵⁵, T. Maier¹⁹, A. Maio^{28,193,229}, K. Maj¹⁷, O. Majersky⁹², S. Majewski⁴⁸, Y. Makida⁷⁸, N. Makovec²⁴, B. Malaescu¹²⁴, Pa. Malecki¹⁰⁰, V. P. Maleev¹¹⁷, F. Malek¹⁸¹, D. Malito^{162,161}, U. Mallik¹⁶⁰, C. Malone¹²¹, S. Maltezos⁴², S. Malyukov³⁰, J. Mamuzic⁷⁹, G. Mancini⁷⁵, I. Mandić¹⁷⁹, L. Manhaes de Andrade Filho⁸⁰, I. M. Maniatis⁹⁸, J. Manjarres Ramos¹³⁴, K. H. Mankinen³⁶, A. Mann¹⁹, A. Manousos²¹¹, B. Mansoulie⁶², I. Manthos⁹⁸, S. Manzoni⁴³, A. Marantis⁹⁸, G. Marceca¹⁸⁷, L. Marchese⁵⁶, G. Marchiori¹²⁴, M. Marcisovsky¹⁷⁸, L. Marcoccia^{33,34}, C. Marcon³⁶, M. Marjanovic², Z. Marshall³², M. U. F. Martensson⁸⁹, S. Marti-Garcia⁷⁹, C. B. Martin¹⁴⁷, T. A. Martin¹²⁶, V. J. Martin¹⁶⁵, B. Martin dit Latour¹⁵⁴, L. Martinelli^{140,159}, M. Martinez^{143,251}, P. Martinez Agullo⁷⁹, V. I. Martinez Outschoorn³, S. Martin-Haugh²², V. S. Martoiu⁴¹, A. C. Martyniuk¹¹³, A. Marzin⁴, S. R. Maschek¹¹⁴, L. Masetti¹⁵, T. Mashimo⁸⁶, R. Mashinistov³⁷, J. Masik¹³⁵, A. L. Maslennikov^{72,71}, L. Massa^{39,38}, P. Massarotti^{50,51}, P. Mastrandrea^{73,139}, A. Mastroberardino^{162,161}, T. Masubuchi⁸⁶, D. Matakias⁹¹, A. Matic¹⁹, N. Matsuzawa⁸⁶, P. Mättig¹⁰⁸,

J. Maurer⁴¹, B. Maček¹⁷⁹, D. A. Maximov^{72,71}, R. Mazini⁴⁵, I. Maznas⁹⁸, S. M. Mazza²³, J. P. Mc Gowan³¹, S. P. Mc Kee⁵⁸, T. G. McCarthy¹¹⁴, W. P. McCormack³², E. F. McDonald¹¹⁰, A. E. McDougall⁴³, J. A. Mcfayden³², G. Mchedlidze¹⁶⁹, M. A. McKay¹³⁶, K. D. McLean⁴⁰, S. J. McMahon²², P. C. McNamara¹¹⁰, C. J. McNicol¹²⁶, R. A. McPherson^{40,244}, J. E. Mdhluli¹⁷⁶, Z. A. Meadows³, S. Meehan⁴, T. Megy²⁵, S. Mehlhase¹⁹, A. Mehta¹⁴⁵, B. Meirose¹⁹⁷, D. Melini¹¹, B. R. Mellado Garcia¹⁷⁶, J. D. Mellenthin⁵, M. Melo⁹², F. Meloni⁵⁹, A. Melzer¹⁰⁸, E. D. Mendes Gouveia^{28,166}, A. M. Mendes Jacques Da Costa⁴⁹, L. Meng⁴, X. T. Meng⁵⁸, S. Menke¹¹⁴, E. Meoni^{162,161}, S. Mergelmeyer⁹⁵, S. A. M. Merkt¹⁰⁷, C. Merlassino⁵⁶, P. Mermod²¹, L. Merola^{50,51}, C. Meroni⁴⁷, G. Merz⁵⁸, O. Meshkov^{206,37}, J. K. R. Meshreki¹²², J. Metcalfe¹², A. S. Mete¹², C. Meyer¹⁵⁸, J.-P. Meyer⁶², M. Michetti⁹⁵, R. P. Middleton²², L. Mijović¹⁶⁵, G. Mikenberg¹⁰⁶, M. Mikestikova¹⁷⁸, M. Mikuž¹⁷⁹, H. Mildner⁶¹, A. Milic⁷, C. D. Milke¹³⁶, D. W. Miller²⁰³, L. S. Miller¹³⁰, A. Milov¹⁰⁶, D. A. Milstead^{65,66}, R. A. Mina¹¹⁵, A. A. Minaenko¹⁴⁶, I. A. Minashvili¹⁶⁹, A. I. Mincer¹⁸⁴, B. Mindur¹⁷, M. Mineev³⁰, Y. Minegishi⁸⁶, Y. Mino³⁵, L. M. Mir¹⁴³, M. Mironova⁵⁶, K. P. Mistry¹⁷¹, T. Mitani²²⁰, J. Mitrevski¹⁹, V. A. Mitsou⁷⁹, M. Mittal¹⁴⁹, O. Miu⁷, A. Miucci⁶⁴, P. S. Miyagawa¹³⁷, A. Mizukami⁷⁸, J. U. Mjörnmark³⁶, T. Mkrtchyan⁶⁸, M. Mlynarikova¹⁸, T. Moa^{65,66}, S. Mobius⁵, K. Mochizuki⁸², P. Mogg¹⁹, S. Mohapatra⁷⁰, R. Moles-Valls¹⁰⁸, K. Mönig⁵⁹, E. Monnier¹, A. Montalbano¹⁰¹, J. Montejo Berlingen⁴, M. Montella¹¹³, F. Monticelli⁵², S. Monzani⁴⁷, N. Morange²⁴, A. L. Moreira De Carvalho²⁸, D. Moreno²³⁰, M. Moreno Llácer⁷⁹, C. Moreno Martinez¹⁴³, P. Morettini¹¹², M. Morgenstern¹¹, S. Morgenstern¹³⁴, D. Mori¹⁰¹, M. Morii⁸⁸, M. Morinaga²²⁰, V. Morisbak¹⁴², A. K. Morley⁴, G. Mornacchi⁴, A. P. Morris¹¹³, L. Morvaj¹²⁹, P. Moschovakos⁴, B. Moser⁴³, M. Mosidze¹⁶⁹, T. Moskalets⁶², P. Moskvitina²⁶, J. Moss^{123,262}, E. J. W. Moyse³, S. Muanza¹, J. Mueller¹⁰⁷, R. S. P. Mueller¹⁹, D. Muenstermann¹¹⁸, G. A. Mullier³⁶, D. P. Mungo^{47,67}, J. L. Munoz Martinez¹⁴³, F. J. Munoz Sanchez¹³⁵, P. Murin¹⁵³, W. J. Murray^{126,22}, A. Murrone^{47,67}, J. M. Muse², M. Muškinja³², C. Mwewa⁹³, A. G. Myagkov^{146,241}, A. A. Myers¹⁰⁷, G. Myers¹⁵⁸, J. Myers⁴⁸, M. Myska⁴⁴, B. P. Nachman³², O. Nackenhorst¹⁸⁶, A. Nag Nag¹³⁴, K. Nagai⁵⁶, K. Nagano⁷⁸, Y. Nagasaka²³¹, J. L. Nagle⁹¹, E. Nagy¹, A. M. Nairz⁴, Y. Nakahama⁸⁴, K. Nakamura⁷⁸, T. Nakamura⁸⁶, H. Nanjo²¹⁶, F. Napolitano⁶⁸, R. F. Naranjo Garcia⁵⁹, R. Narayan¹³⁶, I. Naryshkin¹¹⁷, M. Naseri¹³⁰, T. Naumann⁵⁹, G. Navarro²³⁰, P. Y. Nechaeva³⁷, F. Nechansky⁵⁹, T. J. Neep⁴⁹, A. Negri^{195,196}, M. Negrini³⁹, C. Nellist²⁶, C. Nelson³¹, M. E. Nelson^{65,66}, S. Nemecek¹⁷⁸, M. Nessi^{4,263}, M. S. Neubauer⁹⁴, F. Neuhaus¹⁵, M. Neumann⁹⁶, R. Newhouse¹⁸³, P. R. Newman⁴⁹, C. W. Ng¹⁰⁷, Y. S. Ng⁹⁵, Y. W. Y. Ng⁷⁶, B. Ngair¹²⁰, H. D. N. Nguyen¹, T. Nguyen Manh⁸², E. Nibigira²⁵, R. B. Nickerson⁵⁶, R. Nicolaidou⁶², D. S. Nielsen⁸, J. Nielsen²³, M. Niemeyer⁵, N. Nikiforou⁶³, V. Nikolaenko^{146,241}, I. Nikolic-Audit¹²⁴, K. Nikolopoulos⁴⁹, P. Nilsson⁹¹, H. R. Nindhito²¹, A. Nisati⁷⁷, N. Nishu¹⁴⁹, R. Nisius¹¹⁴, I. Nitsche¹⁸⁶, T. Nitta²²⁰, T. Nobe⁸⁶, D. L. Noel¹²¹, Y. Noguchi³⁵, I. Nomidis¹²⁴, M. A. Nomura⁹¹, M. Nordberg⁴, J. Novak¹⁷⁹, T. Novak¹⁷⁹, O. Novgorodova¹³⁴, R. Novotny⁴⁴, L. Nozka¹⁶⁸, K. Ntekas⁷⁶, E. Nurse¹¹³, F. G. Oakham¹³⁰, H. Oberlack¹¹⁴, J. Ocariz¹²⁴, A. Ochi²¹⁵, I. Ochoa⁷⁰, J. P. Ochoa-Ricoux¹⁸⁹, K. O'Connor⁵⁷, S. Oda²²¹, S. Odaka⁷⁸, S. Oerdek⁵, A. Ogrodnik¹⁷, A. Oh¹³⁵, C. C. Ohm²²⁸, H. Oide⁸⁷, M. L. Ojeda⁷, H. Okawa²¹², Y. Okazaki³⁵, M. W. O'Keefe¹⁴⁵, Y. Okumura⁸⁶, A. Olariu⁴¹, L. F. Oleiro Seabra²⁸, S. A. Olivares Pino¹⁸⁹, D. Oliveira Damazio⁹¹, J. L. Oliver¹⁹², M. J. R. Olsson⁷⁶, A. Olszewski¹⁰⁰, J. Olszowska¹⁰⁰, Ö. O. Öncel¹⁰⁸, D. C. O'Neil¹⁰¹, A. P. O'Neill⁵⁶, A. Onofre^{28,166}, P. U. E. Onyisi⁶³, H. Oppen¹⁴², R. G. Oreamuno Madriz¹⁸, M. J. Oreglia²⁰³, G. E. Orellana⁵², D. Orestano^{140,159}, N. Orlando¹⁴³, R. S. Orr⁷, V. O'Shea¹¹⁹, R. Ospanov¹¹⁶, G. Otero y Garzon¹⁸⁷, H. Otono²²¹, P. S. Ott⁶⁸, G. J. Ottino³², M. Ouchrif⁹⁰, J. Ouellette⁹¹, F. Ould-Saada¹⁴², A. Ouraou^{62,273}, Q. Ouyang⁹⁷, M. Owen¹¹⁹, R. E. Owen²², V. E. Ozcan²⁰, N. Ozturk¹⁰⁴,

J. Pacalt¹⁶⁸, H. A. Pacey¹²¹, K. Pachal⁸¹, A. Pacheco Pages¹⁴³, C. Padilla Aranda¹⁴³, S. Pagan Griso³², G. Palacino¹⁵⁸, S. Palazzo¹⁶⁵, S. Palestini⁴, M. Palka²⁰⁵, P. Palni¹⁷, C. E. Pandini²¹, J. G. Panduro Vazquez⁶, P. Pani⁵⁹, G. Panizzo^{13,180}, L. Paolozzi²¹, C. Papadatos⁸², K. Papageorgiou^{69,248}, S. Parajuli¹³⁶, A. Paramonov¹², C. Paraskevopoulos⁴², D. Paredes Hernandez²²⁷, S. R. Paredes Saenz⁵⁶, B. Parida¹⁰⁶, T. H. Park⁷, A. J. Parker¹²³, M. A. Parker¹²¹, F. Parodi^{112,111}, E. W. Parrish¹⁸, J. A. Parsons⁷⁰, U. Parzefall⁸³, L. Pascual Dominguez¹²⁴, V. R. Pascuzzi³², J. M. P. Pasner²³, F. Pasquali⁴³, E. Pasqualucci⁷⁷, S. Passaggio¹¹², F. Pastore⁶, P. Pasuwan^{65,66}, S. Pataria¹⁵, J. R. Pater¹³⁵, A. Pathak¹⁰⁹, J. Patton¹⁴⁵, T. Pauly⁴, J. Pearkes¹¹⁵, B. Pearson¹¹⁴, M. Pedersen¹⁴², L. Pedraza Diaz²⁶, R. Pedro²⁸, T. Peiffer⁵, S. V. Peleganchuk^{72,71}, O. Penc¹⁷⁸, C. Peng²²⁷, H. Peng¹¹⁶, B. S. Peralva⁸⁰, M. M. Perego²⁴, A. P. Pereira Peixoto²⁸, L. Pereira Sanchez^{65,66}, D. V. Perepelitsa⁹¹, E. Perez Codina¹⁶⁴, F. Peri⁹⁵, L. Perini^{47,67}, H. Pernegger⁴, S. Perrella⁴, A. Perrevoort⁴³, K. Peters⁵⁹, R. F. Y. Peters¹³⁵, B. A. Petersen⁴, T. C. Petersen⁸, E. Petit¹, V. Petousis⁴⁴, C. Petridou⁹⁸, F. Petrucci^{140,159}, M. Pettee¹⁰², N. E. Pettersson³, K. Petukhova¹⁶³, A. Peyaud⁶², R. Pezoa¹⁵², L. Pezzotti^{195,196}, T. Pham¹¹⁰, P. W. Phillips²², M. W. Phipps⁹⁴, G. Piacquadio¹²⁹, E. Pianori³², A. Picazio³, R. H. Pickles¹³⁵, R. Piegaia¹⁸⁷, D. Pietreanu⁴¹, J. E. Pilcher²⁰³, A. D. Pilkington¹³⁵, M. Pinamonti^{13,180}, J. L. Pinfold¹⁴¹, C. Pitman Donaldson¹¹³, M. Pitt¹⁰, L. Pizzimento^{33,34}, A. Pizzini⁴³, M.-A. Pleier⁹¹, V. Plesanovs⁸³, V. Pleskot¹⁶³, E. Plotnikova³⁰, P. Podberezko^{72,71}, R. Poettgen³⁶, R. Poggi²¹, L. Poggioli¹²⁴, I. Pogrebnyak¹⁵¹, D. Pohl¹⁰⁸, I. Pokharel⁵, G. Polesello¹⁹⁵, A. Poley^{101,164}, A. Policicchio^{77,99}, R. Polifka¹⁶³, A. Polini³⁹, C. S. Pollard⁵⁹, V. Polychronakos⁹¹, D. Ponomarenko¹³¹, L. Pontecorvo⁴, S. Popa²³², G. A. Popeneciu²³³, L. Portales¹⁶, D. M. Portillo Quintero¹⁸¹, S. Pospisil⁴⁴, K. Potamianos⁵⁹, I. N. Potrap³⁰, C. J. Potter¹²¹, H. Potti⁶³, T. Poulsen³⁶, J. Poveda⁷⁹, T. D. Powell⁶¹, G. Pownall⁵⁹, M. E. Pozo Astigarraga⁴, A. Prades Ibanez⁷⁹, P. Pralavorio¹, M. M. Prapa¹⁹⁴, S. Prell⁶⁰, D. Price¹³⁵, M. Primavera¹⁷⁵, M. L. Proffitt⁵³, N. Proklova¹³¹, K. Prokofiev²²⁶, F. Prokoshin³⁰, S. Protopopescu⁹¹, J. Proudfoot¹², M. Przybycien¹⁷, D. Pudzha¹¹⁷, A. Puri⁹⁴, P. Puzo²⁴, D. Pyatiizbyantseva¹³¹, J. Qian⁵⁸, Y. Qin¹³⁵, A. Quadt⁵, M. Queitsch-Maitland⁴, M. Racko⁹², F. Ragusa^{47,67}, G. Rahal²³⁴, J. A. Raine²¹, S. Rajagopalan⁹¹, A. Ramirez Morales¹³⁷, K. Ran^{97,177}, D. M. Rauch⁵⁹, F. Rauscher¹⁹, S. Rave¹⁵, B. Ravina¹¹⁹, I. Ravinovitch¹⁰⁶, J. H. Rawling¹³⁵, M. Raymond⁴, A. L. Read¹⁴², N. P. Readoff⁶¹, M. Reale^{175,207}, D. M. Rebuzzi^{195,196}, G. Redlinger⁹¹, K. Reeves¹⁹⁷, D. Reikher¹⁰, A. Reiss¹⁵, A. Rej¹²², C. Rembser⁴, A. Renardi⁵⁹, M. Renda⁴¹, M. B. Rendel¹¹⁴, A. G. Rennie¹¹⁹, S. Resconi⁴⁷, E. D. Resseguie³², S. Rettie¹¹³, B. Reynolds¹⁴⁷, E. Reynolds⁴⁹, O. L. Rezanova^{72,71}, P. Reznicek¹⁶³, E. Ricci^{199,200}, R. Richter¹¹⁴, S. Richter⁵⁹, E. Richter-Was²⁰⁵, M. Ridel¹²⁴, P. Rieck¹¹⁴, O. Rikfi⁵⁹, M. Rijssenbeek¹²⁹, A. Rimoldi^{195,196}, M. Rimoldi⁵⁹, L. Rinaldi³⁹, T. T. Rinn⁹⁴, G. Ripellino²²⁸, I. Riu¹⁴³, P. Rivadeneira⁵⁹, J. C. Rivera Vergara⁴⁰, F. Rizatdinova⁷⁴, E. Rizvi¹³⁷, C. Rizzi⁴, S. H. Robertson^{31,244}, M. Robin⁵⁹, D. Robinson¹²¹, C. M. Robles Gajardo¹⁵², M. Robles Manzano¹⁵, A. Robson¹¹⁹, A. Rocchi^{33,34}, E. Rocco¹⁵, C. Roda^{73,139}, S. Rodriguez Bosca⁷⁹, A. Rodriguez Rodriguez⁸³, A. M. Rodríguez Vera¹⁸⁸, S. Roe⁴, J. Roggel⁹⁶, O. Röhne¹⁴², R. Röhrig¹¹⁴, R. A. Rojas¹⁵², B. Roland⁸³, C. P. A. Roland¹⁵⁸, J. Roloff⁹¹, A. Romaniouk¹³¹, M. Romano^{39,38}, N. Rompotis¹⁴⁵, M. Ronzani¹⁸⁴, L. Roos¹²⁴, S. Rosati⁷⁷, G. Rosin³, B. J. Rosser¹⁷¹, E. Rossi⁵⁹, E. Rossi^{140,159}, E. Rossi^{50,51}, L. P. Rossi¹¹², L. Rossini⁵⁹, R. Rosten¹⁴³, M. Rotaru⁴¹, B. Rottler⁸³, D. Rousseau²⁴, G. Rovelli^{195,196}, A. Roy⁶³, D. Roy¹⁷⁶, A. Rozanov¹, Y. Rozen¹¹, X. Ruan¹⁷⁶, T. A. Ruggeri¹⁹², F. Rühr⁸³, A. Ruiz-Martinez⁷⁹, A. Rummler⁴, Z. Rurikova⁸³, N. A. Rusakovich³⁰, H. L. Russell³¹, L. Rustige^{25,186}, J. P. Rutherford¹³³, E. M. Rüttinger⁶¹, M. Rybar¹⁶³, G. Rybkin²⁴, E. B. Rye¹⁴², A. Ryzhov¹⁴⁶, J. A. Sabater Iglesias⁵⁹, P. Sabatini⁷⁹, L. Sabetta^{77,99}, S. Sacerdoti²⁴, H. F.-W. Sadrozinski²³, R. Sadykov³⁰, F. Safai Tehrani⁷⁷, B. Safarzadeh Samani⁹, M. Safdari¹¹⁵, P. Saha¹⁸, S. Saha³¹, M. Sahinsoy¹¹⁴, A. Sahu⁹⁶, M. Saimpert⁴, M. Saito⁸⁶, T. Saito⁸⁶,

H. Sakamoto⁸⁶, D. Salamani²¹, G. Salamanna^{140,159}, A. Salnikov¹¹⁵, J. Salt⁷⁹, A. Salvador Salas¹⁴³, D. Salvatore^{162,161}, F. Salvatore⁹, A. Salvucci¹⁷³, A. Salzburger⁴, J. Samarati⁴, D. Sammel⁸³, D. Sampsonidis⁹⁸, D. Sampsonidou⁹⁸, J. Sánchez⁷⁹, A. Sanchez Pineda^{13,4,180}, H. Sandaker¹⁴², C. O. Sander⁵⁹, I. G. Sanderswood¹¹⁸, M. Sandhoff⁹⁶, C. Sandoval²³⁵, D. P. C. Sankey²², M. Sannino^{112,111}, Y. Sano⁸⁴, A. Sansoni⁷⁵, C. Santoni²⁵, H. Santos^{28,193}, S. N. Santpur³², A. Santra⁷⁹, K. A. Saoucha⁶¹, A. Sapronov³⁰, J. G. Saraiva^{28,229}, O. Sasaki⁷⁸, K. Sato²¹², F. Sauerburger⁸³, E. Sauvan¹⁶, P. Savard⁷, R. Sawada⁸⁶, C. Sawyer²², L. Sawyer^{236,264}, I. Sayago Galvan⁷⁹, C. Sbarra³⁹, A. Sbrizzi^{13,180}, T. Scanlon¹¹³, J. Schaarschmidt⁵³, P. Schacht¹¹⁴, D. Schaefer²⁰³, L. Schaefer¹⁷¹, U. Schäfer¹⁵, A. C. Schaffer²⁴, D. Schaile¹⁹, R. D. Schamberger¹²⁹, E. Schanet¹⁹, C. Scharf⁹⁵, N. Scharmberg¹³⁵, V. A. Schegelsky¹¹⁷, D. Scheirich¹⁶³, F. Schenck⁹⁵, M. Schernau⁷⁶, C. Schiavi^{112,111}, L. K. Schildgen¹⁰⁸, Z. M. Schillaci⁵⁷, E. J. Schioppa^{175,207}, M. Schioppa^{162,161}, K. E. Schleicher⁸³, S. Schlenker⁴, K. R. Schmidt-Sommerfeld¹¹⁴, K. Schmieden¹⁵, C. Schmitt¹⁵, S. Schmitt⁵⁹, L. Schoeffel⁶², A. Schoening¹⁴⁴, P. G. Scholer⁸³, E. Schopf⁵⁶, M. Schott¹⁵, J. F. P. Schouwenberg²⁶, J. Schovancova⁴, S. Schramm²¹, F. Schroeder⁹⁶, A. Schulte¹⁵, H.-C. Schultz-Coulon⁶⁸, M. Schumacher⁸³, B. A. Schumm²³, Ph. Schune⁶², A. Schwartzman¹¹⁵, T. A. Schwarz⁵⁸, Ph. Schwemling⁶², R. Schwienhorst¹⁵¹, A. Sciandra²³, G. Sciolla⁵⁷, M. Scornajenghi^{162,161}, F. Scuri⁷³, F. Scutti¹¹⁰, L. M. Scyboz¹¹⁴, C. D. Sebastiani¹⁴⁵, P. Seema⁹⁵, S. C. Seidel²¹⁰, A. Seiden²³, B. D. Seidlitz⁹¹, T. Seiss²⁰³, C. Seitz⁵⁹, J. M. Seixas⁵⁵, G. Sekhniaidze⁵⁰, S. J. Sekula¹³⁶, N. Semprini-Cesari^{39,38}, S. Sen⁸¹, C. Serfon⁹¹, L. Serin²⁴, L. Serkin^{13,14}, M. Sessa¹¹⁶, H. Severini², S. Sevova¹¹⁵, F. Sforza^{112,111}, A. Sfyrila²¹, E. Shabalina⁵, J. D. Shahinian¹⁷¹, N. W. Shaikh^{65,66}, D. Shaked Renous¹⁰⁶, L. Y. Shan⁹⁷, M. Shapiro³², A. Sharma⁴, A. S. Sharma¹⁹², P. B. Shatalov²⁰⁴, K. Shaw⁹, S. M. Shaw¹³⁵, M. Shehade¹⁰⁶, Y. Shen², A. D. Sherman¹⁵⁵, P. Sherwood¹¹³, L. Shi¹¹³, C. O. Shimmin¹⁰², Y. Shimogama²²⁰, M. Shimojima²⁰², J. D. Shinner⁶, I. P. J. Shipsey⁵⁶, S. Shirabe⁸⁷, M. Shiyakova^{30,265}, J. Shlomi¹⁰⁶, A. Shmeleva³⁷, M. J. Shochet²⁰³, J. Shojaii¹¹⁰, D. R. Shope²²⁸, S. Shrestha¹⁴⁷, E. M. Shrif¹⁷⁶, M. J. Shroff⁴⁰, E. Shulga¹⁰⁶, P. Sicho¹⁷⁸, A. M. Sickles⁹⁴, E. Sideras Haddad¹⁷⁶, O. Sidiropoulou⁴, A. Sidoti^{39,38}, F. Siegert¹³⁴, Dj. Sijacki¹⁰³, M. Jr. Silva¹⁰⁹, M. V. Silva Oliveira⁴, S. B. Silverstein⁶⁵, S. Simion²⁴, R. Simoniello¹⁵, C. J. Simpson-allso⁴⁹, S. Simsek¹⁶⁷, P. Sinervo⁷, V. Sinetckii²⁰⁶, S. Singh¹⁰¹, M. Sioli^{39,38}, I. Siral⁴⁸, S. Yu. Sivoklov²⁰⁶, J. Sjölin^{65,66}, A. Skaf⁵, E. Skorda³⁶, P. Skubic², M. Slawinska¹⁰⁰, K. Sliwa¹²⁵, R. Slovak¹⁶³, V. Smakhtin¹⁰⁶, B. H. Smart²², J. Smiesko¹⁵³, N. Smirnov¹³¹, S. Yu. Smirnov¹³¹, Y. Smirnov¹³¹, L. N. Smirnova^{206,266}, O. Smirnova³⁶, E. A. Smith²⁰³, H. A. Smith⁵⁶, M. Smizanska¹¹⁸, K. Smolek⁴⁴, A. Smykiewicz¹⁰⁰, A. A. Snegarev³⁷, H. L. Snoek⁴³, I. M. Snyder⁴⁸, S. Snyder⁹¹, R. Sobie^{40,244}, A. Soffer¹⁰, A. Søgaard¹⁶⁵, F. Sohns⁵, C. A. Solans Sanchez⁴, E. Yu. Soldatov¹³¹, U. Soldevila⁷⁹, A. A. Solodkov¹⁴⁶, A. Soloshenko³⁰, O. V. Solovyanov¹⁴⁶, V. Solovyev¹¹⁷, P. Sommer⁶¹, H. Son¹²⁵, A. Sonay¹⁴³, W. Song²², W. Y. Song¹⁸⁸, A. Sopczak⁴⁴, A. L. Sopio¹¹³, F. Sopkova¹⁵³, S. Sottocornola^{195,196}, R. Soualah^{13,180}, A. M. Soukharev^{72,71}, D. South⁵⁹, S. Spagnolo^{175,207}, M. Spalla¹¹⁴, M. Spangenberg¹²⁶, F. Spanò⁶, D. Sperlich⁸³, T. M. Spieker⁶⁸, G. Spigo⁴, M. Spina⁹, D. P. Spiteri¹¹⁹, M. Spousta¹⁶³, A. Stabile^{47,67}, B. L. Stamas¹⁸, R. Stamen⁶⁸, M. Stamenkovic⁴³, A. Stampekis⁴⁹, E. Stanecka¹⁰⁰, B. Stanislaus⁵⁶, M. M. Stanitzki⁵⁹, M. Stankaityte⁵⁶, B. Stapf⁴³, E. A. Starchenko¹⁴⁶, G. H. Stark²³, J. Stark¹⁸¹, P. Staroba¹⁷⁸, P. Starovoitov⁶⁸, S. Stärz³¹, R. Staszewski¹⁰⁰, G. Stavropoulos¹⁹⁴, M. Stegler⁵⁹, P. Steinberg⁹¹, A. L. Steinhebel⁴⁸, B. Stelzer^{101,164}, H. J. Stelzer¹⁰⁷, O. Stelzer-Chilton¹⁶⁴, H. Stenzel¹⁵⁶, T. J. Stevenson⁹, G. A. Stewart⁴, M. C. Stockton⁴, G. Stoicea⁴¹, M. Stolarski²⁸, S. Stonjek¹¹⁴, A. Straessner¹³⁴, J. Strandberg²²⁸, S. Strandberg^{65,66}, M. Strauss², T. Streblor¹, P. Strizenec¹⁵³, R. Ströhmer¹³⁸, D. M. Strom⁴⁸, R. Stroynowski¹³⁶, A. Strubig^{65,66}, S. A. Stucci⁹¹, B. Stugu¹⁵⁴, J. Stupak², N. A. Styles⁵⁹, D. Su¹¹⁵, W. Su^{149,53}, X. Su¹¹⁶,

V. V. Sulin³⁷, M. J. Sullivan¹⁴⁵, D. M. S. Sultan²¹, S. Sultansoy²³⁷, T. Sumida³⁵, S. Sun⁵⁸, X. Sun¹³⁵, C. J. E. Suster¹⁰⁵, M. R. Sutton⁹, S. Suzuki⁷⁸, M. Svatos¹⁷⁸, M. Swiatlowski¹⁶⁴, S. P. Swift²¹⁸, T. Swirski¹³⁸, A. Sydorenko¹⁵, I. Sykora⁹², M. Sykora¹⁶³, T. Sykora¹⁶³, D. Ta¹⁵, K. Tackmann^{59,267}, J. Taenzer¹⁰, A. Taffard⁷⁶, R. Tafirout¹⁶⁴, E. Tagiev¹⁴⁶, R. Takashima²³⁸, K. Takeda²¹⁵, T. Takeshita²¹⁴, E. P. Takeva¹⁶⁵, Y. Takubo⁷⁸, M. Talby¹, A. A. Talyshev^{72,71}, K. C. Tam²²⁷, N. M. Tamir¹⁰, J. Tanaka⁸⁶, R. Tanaka²⁴, S. Tapia Araya⁹⁴, S. Tapprogge¹⁵, A. Tarek Abouelfadl Mohamed¹⁵¹, S. Tarem¹¹, K. Tariq¹⁸⁵, G. Tarna^{41,268}, G. F. Tartarelli⁴⁷, P. Tas¹⁶³, M. Tasevsky¹⁷⁸, E. Tassi^{162,161}, A. Tavares Delgado²⁸, Y. Tayalati¹²⁰, A. J. Taylor¹⁶⁵, G. N. Taylor¹¹⁰, W. Taylor¹⁸⁸, H. Teagle¹⁴⁵, A. S. Tee¹¹⁸, R. Teixeira De Lima¹¹⁵, P. Teixeira-Dias⁶, H. Ten Kate⁴, J. J. Teoh⁴³, K. Terashi¹⁸⁶, J. Terron⁵⁴, S. Terzo¹⁴³, M. Testa⁷⁵, R. J. Teuscher^{7,244}, S. J. Thais¹⁰², N. Themistokleous¹⁶⁵, T. Theveneaux-Pelzer⁵⁹, F. Thiele⁸, D. W. Thomas⁶, J. O. Thomas¹³⁶, J. P. Thomas⁴⁹, E. A. Thompson⁵⁹, P. D. Thompson⁴⁹, E. Thomson¹⁷¹, E. J. Thorpe¹³⁷, R. E. Ticse Torres⁵, V. O. Tikhomirov^{37,269}, Yu. A. Tikhonov^{72,71}, S. Timoshenko¹³¹, P. Tipton¹⁰², S. Tisserant¹, K. Todome^{39,38}, S. Todorova-Nova¹⁶³, S. Todt¹³⁴, J. Tojo²²¹, S. Tokár⁹², K. Tokushuku⁷⁸, E. Tolley¹⁴⁷, R. Tombs¹²¹, K. G. Tomiwa¹⁷⁶, M. Tomoto^{78,84}, L. Tompkins¹¹⁵, P. Tornambe³, E. Torrence⁴⁸, H. Torres¹³⁴, E. Torró Pastor⁷⁹, M. Toscani¹⁸⁷, C. Tosciri⁵⁶, J. Toth^{1,270}, D. R. Tovey⁶¹, A. Traeet¹⁵⁴, C. J. Treado¹⁸⁴, T. Trefzger¹³⁸, F. Tresoldi⁹, A. Tricoli⁹¹, I. M. Trigger¹⁶⁴, S. Trincaz-Duvoid¹²⁴, D. A. Trischuk¹⁸³, W. Trischuk⁷, B. Trocme¹⁸¹, A. Trofymov²⁴, C. Troncon⁴⁷, F. Trovato⁹, L. Truong¹⁴⁸, M. Trzebinski¹⁰⁰, A. Trzupek¹⁰⁰, F. Tsai⁵⁹, J. C.-L. Tseng⁵⁶, P. V. Tsiareshka^{213,258}, A. Tsirigotis^{98,259}, V. Tsiskaridze¹²⁹, E. G. Tskhadadze²¹⁹, M. Tsopoulou⁹⁸, I. I. Tsukerman²⁰⁴, V. Tsulaia³², S. Tsuno⁷⁸, D. Tsybychev¹²⁹, Y. Tu²²⁷, A. Tudorache⁴¹, V. Tudorache⁴¹, T. T. Tulbure²³², A. N. Tuna⁸⁸, S. Turchikhin³⁰, D. Turgeman¹⁰⁶, I. Turk Cakir^{223,271}, R. J. Turner⁴⁹, R. Turra⁴⁷, P. M. Tuts⁷⁰, S. Tzamarias⁹⁸, E. Tzovara¹⁵, K. Uchida⁸⁶, F. Ukegawa²¹², G. Unal⁴, M. Unal⁶³, A. Undrus⁹¹, G. Unel⁷⁶, F. C. Ungaro¹¹⁰, Y. Unno⁷⁸, K. Uno⁸⁶, J. Urban¹⁵³, P. Urquijo¹¹⁰, G. Usai¹⁰⁴, Z. Uysal¹²⁷, V. Vacek⁴⁴, B. Vachon³¹, K. O. H. Vadla¹⁴², T. Vafeiadis⁴, A. Vaidya¹¹³, C. Valderanis¹⁹, E. Valdes Santurio^{65,66}, M. Valente¹⁶⁴, S. Valentini^{39,38}, A. Valero⁷⁹, L. Valéry⁵⁹, R. A. Vallance⁴⁹, A. Vallier⁴, J. A. Valls Ferrer⁷⁹, T. R. Van Daalen¹⁴³, P. Van Gemmeren¹², S. Van Stroud¹¹³, I. Van Vulpen⁴³, M. Vanadia^{33,34}, W. Vandelli⁴, M. Vandenbroucke⁶², E. R. Vandewall⁷⁴, A. Vaniachine⁴⁶, D. Vannicola^{77,99}, R. Vari⁷⁷, E. W. Varnes¹³³, C. Varni^{112,111}, T. Varol⁴⁵, D. Varouchas²⁴, K. E. Varvell¹⁰⁵, M. E. Vasile⁴¹, G. A. Vasquez⁴⁰, F. Vazeille²⁵, D. Vazquez Furelos¹⁴³, T. Vazquez Schroeder⁴, J. Veatch⁵, V. Vecchio¹³⁵, M. J. Veen⁴³, L. M. Veloce⁷, F. Veloso^{28,198}, S. Veneziano⁷⁷, A. Ventura^{175,207}, A. Verbytskyi¹¹⁴, V. Vercesi¹⁹⁵, M. Verducci^{73,139}, C. M. Vergel Infante⁶⁰, C. Vergis¹⁰⁸, W. Verkerke⁴³, A. T. Vermeulen⁴³, J. C. Vermeulen⁴³, C. Vernieri¹¹⁵, P. J. Verschuuren⁶, M. C. Vetterli¹⁰¹, N. Viaux Maira¹⁵², T. Vickey⁶¹, O. E. Vickey Boeriu⁶¹, G. H. A. Viehhauser⁵⁶, L. Viganì¹⁴⁴, M. Villa^{39,38}, M. Villaplana Perez¹⁴¹, E. M. Villhauer¹⁶⁵, E. Vilucchi⁷⁵, M. G. Vinciter¹³⁰, G. S. Virdee⁴⁹, A. Vishwakarma¹⁶⁵, C. Vittori^{39,38}, I. Vivarelli⁹, M. Vogel⁹⁶, P. Vokac⁴⁴, S. E. von Buddenbrock¹⁷⁶, E. Von Toerne¹⁰⁸, V. Vorobel¹⁶³, K. Vorobev¹³¹, M. Vos⁷⁹, J. H. Vossebeld¹⁴⁵, M. Vozak¹³⁵, N. Vranjes¹⁰³, M. Vranjes Milosavljevic¹⁰³, V. Vrba^{44,273}, M. Vreeswijk⁴³, N. K. Vu¹, R. Vuillermet⁴, I. Vukotic²⁰³, S. Wada²¹², P. Wagner¹⁰⁸, W. Wagner⁹⁶, J. Wagner-Kuhr¹⁹, S. Wahdan⁹⁶, H. Wahlberg⁵², R. Wakasa²¹², V. M. Walbrecht¹¹⁴, J. Walder²², R. Walker¹⁹, S. D. Walker⁶, W. Walkowiak¹²², V. Wallangen^{65,66}, A. M. Wang⁸⁸, A. Z. Wang¹⁰⁹, C. Wang¹¹⁶, C. Wang¹⁴⁹, F. Wang¹⁰⁹, H. Wang³², H. Wang¹⁴¹, J. Wang¹⁷³, P. Wang¹³⁶, Q. Wang², R.-J. Wang¹⁵, R. Wang¹¹⁶, R. Wang¹², S. M. Wang⁴⁵, W. T. Wang¹¹⁶, W. Wang¹⁷⁰, W. X. Wang¹¹⁶, Y. Wang¹¹⁶, Z. Wang⁵⁸, C. Wanotayaroj⁵⁹, A. Warburton³¹, C. P. Ward¹²¹, R. J. Ward⁴⁹, N. Warrack¹¹⁹, A. T. Watson⁴⁹, M. F. Watson⁴⁹, G. Watts⁵³, B. M. Waugh¹¹³, A. F. Webb⁶³, C. Weber⁹¹, M. S. Weber⁶⁴, S. A. Weber¹³⁰, S. M. Weber⁶⁸,

A. R. Weidberg⁵⁶, J. Weingarten¹⁸⁶, M. Weirich¹⁵, C. Weiser⁸³, P. S. Wells⁴, T. Wenaus⁹¹, B. Wendland¹⁸⁶, T. Wengler⁴, S. Wenig⁴, N. Wermes¹⁰⁸, M. Wessels⁶⁸, T. D. Weston⁶⁴, K. Whalen⁴⁸, A. M. Wharton¹¹⁸, A. S. White⁵⁸, A. White¹⁰⁴, M. J. White¹⁹², D. Whiteson⁷⁶, B. W. Whitmore¹¹⁸, W. Wiedenmann¹⁰⁹, C. Wiel¹³⁴, M. WIELERS²², N. Wieseotte¹⁵, C. Wigglesworth⁸, L. A. M. Wiik-Fuchs⁸³, H. G. Wilkens⁴, L. J. Wilkins⁶, H. H. Williams¹⁷¹, S. Williams¹²¹, S. Willocq³, P. J. Windischhofer⁵⁶, I. Wingerter-Seez¹⁶, E. Winkels⁹, F. Winklmeier⁴⁸, B. T. Winter⁸³, M. Wittgen¹¹⁵, M. Wobisch²³⁶, A. Wolf¹⁵, R. Wölker⁵⁶, J. Wollrath⁸³, M. W. Wolter¹⁰⁰, H. Wolters^{28,198}, V. W. S. Wong¹⁸³, N. L. Woods²³, S. D. Worm⁵⁹, B. K. Wosiek¹⁰⁰, K. W. Woźniak¹⁰⁰, K. Wraight¹¹⁹, S. L. Wu¹⁰⁹, X. Wu²¹, Y. Wu¹¹⁶, J. Wuerzinger⁵⁶, T. R. Wyatt¹³⁵, B. M. Wynne¹⁶⁵, S. Xella⁸, J. Xiang²²⁶, X. Xiao⁵⁸, X. Xie¹¹⁶, I. Xiotidis⁹, D. Xu⁹⁷, H. Xu¹¹⁶, H. Xu¹¹⁶, L. Xu⁹¹, T. Xu⁶², W. Xu⁵⁸, Y. Xu¹⁷², Z. Xu¹⁸⁵, Z. Xu¹¹⁵, B. Yabsley¹⁰⁵, S. Yacoub⁹³, D. P. Yallup¹¹³, N. Yamaguchi²²¹, Y. Yamaguchi⁸⁷, A. Yamamoto⁷⁸, M. Yamatani⁸⁶, T. Yamazaki⁸⁶, Y. Yamazaki²¹⁵, J. Yan¹⁴⁹, Z. Yan¹⁵⁵, H. J. Yang^{149,150}, H. T. Yang³², S. Yang¹¹⁶, T. Yang²²⁶, X. Yang^{185,181}, Y. Yang⁸⁶, Z. Yang¹¹⁶, W.-M. Yao³², Y. C. Yap⁵⁹, E. Yatsenko¹⁴⁹, H. Ye¹⁷⁰, J. Ye¹³⁶, S. Ye⁹¹, I. Yeletsikh³⁰, M. R. Yexley¹¹⁸, E. Yigitbasi¹⁵⁵, P. Yin⁷⁰, K. Yorita²²⁰, K. Yoshihara⁶⁰, C. J. S. Young⁴, C. Young¹¹⁵, J. Yu⁶⁰, R. Yuan^{185,272}, X. Yue⁶⁸, M. Zaazoua¹²⁰, B. Zabinski¹⁰⁰, G. Zacharis⁴², E. Zaffaroni²¹, J. Zahreddine¹²⁴, A. M. Zaitsev^{146,241}, T. Zakareishvili¹⁶⁹, N. Zakharchuk¹³⁰, S. Zambito⁴, D. Zanzi⁴, S. V. Zeißner¹⁸⁶, C. Zeitnitz⁹⁶, G. Zemaityte⁵⁶, J. C. Zeng⁹⁴, O. Zenin¹⁴⁶, T. Ženiš⁹², D. Zerwas²⁴, M. Zgubič⁵⁶, B. Zhang¹⁷⁰, D. F. Zhang¹⁷², G. Zhang¹⁷², J. Zhang¹², K. Zhang⁹⁷, L. Zhang¹⁷⁰, L. Zhang¹¹⁶, M. Zhang⁹⁴, R. Zhang¹⁰⁹, S. Zhang⁵⁸, X. Zhang¹⁴⁹, X. Zhang¹⁸⁵, Y. Zhang^{97,177}, Z. Zhang¹⁷³, Z. Zhang²⁴, P. Zhao⁸¹, Z. Zhao¹¹⁶, A. Zhemchugov³⁰, Z. Zheng⁵⁸, D. Zhong⁹⁴, B. Zhou⁵⁸, C. Zhou¹⁰⁹, H. Zhou¹³³, M. S. Zhou^{97,177}, M. Zhou¹²⁹, N. Zhou¹⁴⁹, Y. Zhou¹³³, C. G. Zhu¹⁸⁵, C. Zhu^{97,177}, H. L. Zhu¹¹⁶, H. Zhu⁹⁷, J. Zhu⁵⁸, Y. Zhu¹¹⁶, X. Zhuang⁹⁷, K. Zhukov³⁷, V. Zhulanov^{72,71}, D. Zieminska¹⁵⁸, N. I. Zimine³⁰, S. Zimmermann^{83,273}, Z. Zinonos¹¹⁴, M. Ziolkowski¹²², L. Živković¹⁰³, G. Zobernig¹⁰⁹, A. Zoccoli^{39,38}, K. Zoch⁵, T. G. Zorbas⁶¹, R. Zou²⁰³ and L. Zwalinski⁴

¹CPPM, Aix-Marseille Université, CNRS/IN2P3, Marseille, France. ²Homer L. Dodge Department of Physics and Astronomy, University of Oklahoma, Norman, OK, USA. ³Department of Physics, University of Massachusetts, Amherst, MA, USA. ⁴CERN, Geneva, Switzerland. ⁵Il. Physikalisches Institut, Georg-August-Universität Göttingen, Göttingen, Germany. ⁶Department of Physics, Royal Holloway University of London, Egham, UK. ⁷Department of Physics, University of Toronto, Toronto, Ontario, Canada. ⁸Niels Bohr Institute, University of Copenhagen, Copenhagen, Denmark. ⁹Department of Physics and Astronomy, University of Sussex, Brighton, UK. ¹⁰Raymond and Beverly Sackler School of Physics and Astronomy, Tel Aviv University, Tel Aviv, Israel. ¹¹Department of Physics, Technion, Israel Institute of Technology, Haifa, Israel. ¹²High Energy Physics Division, Argonne National Laboratory, Argonne, IL, USA. ¹³INFN Gruppo Collegato di Udine, Sezione di Trieste, Udine, Italy. ¹⁴ICTP, Trieste, Italy. ¹⁵Institut für Physik, Universität Mainz, Mainz, Germany. ¹⁶LAPP, Université Grenoble Alpes, Université Savoie Mont Blanc, CNRS/IN2P3, Annecy, France. ¹⁷AGH University of Science and Technology, Faculty of Physics and Applied Computer Science, Krakow, Poland. ¹⁸Department of Physics, Northern Illinois University, DeKalb, IL, USA. ¹⁹Fakultät für Physik, Ludwig-Maximilians-Universität München, Munich, Germany. ²⁰Department of Physics, Bogazici University, Istanbul, Turkey. ²¹Département de Physique Nucléaire et Corpusculaire, Université de Genève, Geneva, Switzerland. ²²Particle Physics Department, Rutherford Appleton Laboratory, Didcot, UK. ²³Santa Cruz Institute for Particle Physics, University of California Santa Cruz, Santa Cruz, CA, USA. ²⁴IJCLab, Université Paris-Saclay, CNRS/IN2P3, 91405, Orsay, France. ²⁵LPC, Université Clermont Auvergne, CNRS/IN2P3, Clermont-Ferrand, France. ²⁶Institute for Mathematics, Astrophysics and Particle Physics, Radboud University/Nikhef, Nijmegen, Netherlands. ²⁷Department of Physics, Alexandru Ioan Cuza University of Iasi, Iasi, Romania. ²⁸Laboratório de Instrumentação e Física Experimental de Partículas – LIP, Lisbon, Portugal. ²⁹Departamento de Física Teórica y del Cosmos, Universidad de Granada, Granada, Spain. ³⁰Joint Institute for Nuclear Research, Dubna, Russia. ³¹Department of Physics, McGill University, Montreal, Quebec, Canada. ³²Physics Division, Lawrence Berkeley National Laboratory and University of California, Berkeley, CA, USA. ³³INFN Sezione di Roma Tor Vergata, Rome, Italy. ³⁴Dipartimento di Fisica, Università di Roma Tor Vergata, Rome, Italy. ³⁵Faculty of Science, Kyoto University, Kyoto, Japan. ³⁶Fysiska Institutionen, Lunds Universitet, Lund, Sweden. ³⁷P.N. Lebedev Physical Institute of the Russian Academy of Sciences, Moscow, Russia. ³⁸Dipartimento di Fisica, INFN Bologna and Università di Bologna, Bologna, Italy. ³⁹INFN Sezione di Bologna, Bologna, Italy. ⁴⁰Department of Physics and Astronomy, University of Victoria, Victoria, British Columbia, Canada. ⁴¹Horia Hulubei National Institute of Physics and Nuclear Engineering, Bucharest, Romania. ⁴²Physics Department, National Technical University of Athens, Zografou, Greece. ⁴³Nikhef National Institute for Subatomic Physics and University of Amsterdam, Amsterdam, Netherlands. ⁴⁴Czech Technical University in Prague, Prague, Czech Republic. ⁴⁵Institute of Physics, Academia Sinica, Taipei, Taiwan. ⁴⁶Tomsk State University, Tomsk, Russia. ⁴⁷INFN Sezione di Milano, Milan, Italy. ⁴⁸Institute for Fundamental Science, University of Oregon, Eugene, OR, USA. ⁴⁹School of Physics and Astronomy, University of Birmingham, Birmingham, UK. ⁵⁰INFN Sezione di Napoli, Naples, Italy. ⁵¹Dipartimento di Fisica, Università di Napoli, Naples, Italy. ⁵²Instituto de Física La Plata, Universidad Nacional de La Plata and CONICET, La Plata, Argentina. ⁵³Department of Physics, University of Washington, Seattle, WA, USA. ⁵⁴Departamento de Física Teórica C-15 and CIAFF, Universidad Autónoma de Madrid, Madrid, Spain. ⁵⁵Universidade Federal do Rio de Janeiro COPPE/EE/IF, Rio de Janeiro, Brazil. ⁵⁶Department of Physics, Oxford University, Oxford, UK. ⁵⁷Department of Physics, Brandeis University, Waltham, MA, USA. ⁵⁸Department of Physics, University of Michigan, Ann Arbor, MI, USA. ⁵⁹Deutsches Elektronen-Synchrotron DESY,

Hamburg and Zeuthen, Germany. ⁶⁰Department of Physics and Astronomy, Iowa State University, Ames, IA, USA. ⁶¹Department of Physics and Astronomy, University of Sheffield, Sheffield, UK. ⁶²IRFU, CEA, Université Paris-Saclay, Gif-sur-Yvette, France. ⁶³Department of Physics, University of Texas at Austin, Austin, TX, USA. ⁶⁴Albert Einstein Center for Fundamental Physics and Laboratory for High Energy Physics, University of Bern, Bern, Switzerland. ⁶⁵Department of Physics, Stockholm University, Stockholm, Sweden. ⁶⁶Oskar Klein Centre, Stockholm, Sweden. ⁶⁷Dipartimento di Fisica, Università di Milano, Milan, Italy. ⁶⁸Kirchhoff-Institut für Physik, Ruprecht-Karls-Universität Heidelberg, Heidelberg, Germany. ⁶⁹Physics Department, National and Kapodistrian University of Athens, Athens, Greece. ⁷⁰Nevis Laboratory, Columbia University, Irvington, NY, USA. ⁷¹Budker Institute of Nuclear Physics and NSU, SB RAS, Novosibirsk, Russia. ⁷²Novosibirsk State University Novosibirsk, Novosibirsk, Russia. ⁷³INFN Sezione di Pisa, Pisa, Italy. ⁷⁴Department of Physics, Oklahoma State University, Stillwater, OK, USA. ⁷⁵INFN e Laboratori Nazionali di Frascati, Frascati, Italy. ⁷⁶Department of Physics and Astronomy, University of California Irvine, Irvine, CA, USA. ⁷⁷INFN Sezione di Roma, Rome, Italy. ⁷⁸KEK, High Energy Accelerator Research Organization, Tsukuba, Japan. ⁷⁹Instituto de Física Corpuscular (IFIC), Centro Mixto Universidad de Valencia – CSIC, Valencia, Spain. ⁸⁰Departamento de Engenharia Elétrica, Universidade Federal de Juiz de Fora (UFJF), Juiz de Fora, Brazil. ⁸¹Department of Physics, Duke University, Durham, NC, USA. ⁸²Group of Particle Physics, University of Montreal, Montreal, Quebec, Canada. ⁸³Physikalisches Institut, Albert-Ludwigs-Universität Freiburg, Freiburg, Germany. ⁸⁴Graduate School of Science and Kobayashi-Maskawa Institute, Nagoya University, Nagoya, Japan. ⁸⁵Ochanomizu University, Tokyo, Japan. ⁸⁶International Center for Elementary Particle Physics and Department of Physics, University of Tokyo, Tokyo, Japan. ⁸⁷Department of Physics, Tokyo Institute of Technology, Tokyo, Japan. ⁸⁸Laboratory for Particle Physics and Cosmology, Harvard University, Cambridge, MA, USA. ⁸⁹Department of Physics and Astronomy, University of Uppsala, Uppsala, Sweden. ⁹⁰LPMR, Faculté des Sciences, Université Mohamed Premier, Oujda, Morocco. ⁹¹Physics Department, Brookhaven National Laboratory, Upton, NY, USA. ⁹²Faculty of Mathematics, Physics and Informatics, Comenius University, Bratislava, Slovakia. ⁹³Department of Physics, University of Cape Town, Cape Town, South Africa. ⁹⁴Department of Physics, University of Illinois, Urbana, IL, USA. ⁹⁵Institut für Physik, Humboldt Universität zu Berlin, Berlin, Germany. ⁹⁶Fakultät für Mathematik und Naturwissenschaften, Fachgruppe Physik, Bergische Universität Wuppertal, Wuppertal, Germany. ⁹⁷Institute of High Energy Physics, Chinese Academy of Sciences, Beijing, China. ⁹⁸Department of Physics, Aristotle University of Thessaloniki, Thessaloniki, Greece. ⁹⁹Dipartimento di Fisica, Sapienza Università di Roma, Rome, Italy. ¹⁰⁰Institute of Nuclear Physics Polish Academy of Sciences, Krakow, Poland. ¹⁰¹Department of Physics, Simon Fraser University, Burnaby, British Columbia, Canada. ¹⁰²Department of Physics, Yale University, New Haven, CT, USA. ¹⁰³Institute of Physics, University of Belgrade, Belgrade, Serbia. ¹⁰⁴Department of Physics, University of Texas at Arlington, Arlington, TX, USA. ¹⁰⁵School of Physics, University of Sydney, Sydney, Australia. ¹⁰⁶Department of Particle Physics and Astrophysics, Weizmann Institute of Science, Rehovot, Israel. ¹⁰⁷Department of Physics and Astronomy, University of Pittsburgh, Pittsburgh, PA, USA. ¹⁰⁸Physikalisches Institut, Universität Bonn, Bonn, Germany. ¹⁰⁹Department of Physics, University of Wisconsin, Madison, WI, USA. ¹¹⁰School of Physics, University of Melbourne, Melbourne, Victoria, Australia. ¹¹¹Dipartimento di Fisica, Università di Genova, Genova, Italy. ¹¹²INFN Sezione di Genova, Genova, Italy. ¹¹³Department of Physics and Astronomy, University College London, London, UK. ¹¹⁴Max-Planck-Institut für Physik (Werner-Heisenberg-Institut), Munich, Germany. ¹¹⁵SLAC National Accelerator Laboratory, Stanford, CA, USA. ¹¹⁶Department of Modern Physics and State Key Laboratory of Particle Detection and Electronics, University of Science and Technology of China, Hefei, China. ¹¹⁷Konstantinov Nuclear Physics Institute of National Research Centre 'Kurchatov Institute', PNPI, St Petersburg, Russia. ¹¹⁸Physics Department, Lancaster University, Lancaster, UK. ¹¹⁹SUPA – School of Physics and Astronomy, University of Glasgow, Glasgow, UK. ¹²⁰Faculté des Sciences, Université Mohammed V, Rabat, Morocco. ¹²¹Cavendish Laboratory, University of Cambridge, Cambridge, UK. ¹²²Department Physik, Universität Siegen, Siegen, Germany. ¹²³California State University, Long Beach, CA, USA. ¹²⁴LPNHE, Sorbonne Université, Université de Paris, CNRS/IN2P3, Paris, France. ¹²⁵Department of Physics and Astronomy, Tufts University, Medford, MA, USA. ¹²⁶Department of Physics, University of Warwick, Coventry, UK. ¹²⁷Department of Physics Engineering, Gaziantep University, Gaziantep, Turkey. ¹²⁸Bahcesehir University, Faculty of Engineering and Natural Sciences, Istanbul, Turkey. ¹²⁹Departments of Physics and Astronomy, Stony Brook University, Stony Brook, NY, USA. ¹³⁰Department of Physics, Carleton University, Ottawa, Ontario, Canada. ¹³¹National Research Nuclear University MEPhI, Moscow, Russia. ¹³²Faculté des Sciences Ain Chock, Réseau Universitaire de Physique des Hautes Energies – Université Hassan II, Casablanca, Morocco. ¹³³Department of Physics, University of Arizona, Tucson, AZ, USA. ¹³⁴Institut für Kern- und Teilchenphysik, Technische Universität Dresden, Dresden, Germany. ¹³⁵School of Physics and Astronomy, University of Manchester, Manchester, UK. ¹³⁶Physics Department, Southern Methodist University, Dallas, TX, USA. ¹³⁷School of Physics and Astronomy, Queen Mary University of London, London, UK. ¹³⁸Fakultät für Physik und Astronomie, Julius-Maximilians-Universität Würzburg, Würzburg, Germany. ¹³⁹Dipartimento di Fisica E. Fermi, Università di Pisa, Pisa, Italy. ¹⁴⁰INFN Sezione di Roma Tre, Rome, Italy. ¹⁴¹Department of Physics, University of Alberta, Edmonton, Alberta, Canada. ¹⁴²Department of Physics, University of Oslo, Oslo, Norway. ¹⁴³Institut de Física d'Altes Energies (IFAE), Barcelona Institute of Science and Technology, Barcelona, Spain. ¹⁴⁴Physikalisches Institut, Ruprecht-Karls-Universität Heidelberg, Heidelberg, Germany. ¹⁴⁵Oliver Lodge Laboratory, University of Liverpool, Liverpool, UK. ¹⁴⁶Institute for High Energy Physics of the National Research Centre Kurchatov Institute, Protvino, Russia. ¹⁴⁷Ohio State University, Columbus, OH, USA. ¹⁴⁸Department of Mechanical Engineering Science, University of Johannesburg, Johannesburg, South Africa. ¹⁴⁹School of Physics and Astronomy, Shanghai Jiao Tong University, Key Laboratory for Particle Astrophysics and Cosmology (MOE), SKLPPC, Shanghai, China. ¹⁵⁰Tsung-Dao Lee Institute, Shanghai, China. ¹⁵¹Department of Physics and Astronomy, Michigan State University, East Lansing, MI, USA. ¹⁵²Departamento de Física, Universidad Técnica Federico Santa María, Valparaíso, Chile. ¹⁵³Department of Subnuclear Physics, Institute of Experimental Physics of the Slovak Academy of Sciences, Kosice, Slovak Republic. ¹⁵⁴Department for Physics and Technology, University of Bergen, Bergen, Norway. ¹⁵⁵Department of Physics, Boston University, Boston, MA, USA. ¹⁵⁶II. Physikalisches Institut, Justus-Liebig-Universität Giessen, Giessen, Germany. ¹⁵⁷Department of Physics, Ankara University, Ankara, Turkey. ¹⁵⁸Department of Physics, Indiana University, Bloomington, IN, USA. ¹⁵⁹Dipartimento di Matematica e Fisica, Università Roma Tre, Rome, Italy. ¹⁶⁰University of Iowa, Iowa City, IA, USA. ¹⁶¹Dipartimento di Fisica, Università della Calabria, Rende, Italy. ¹⁶²INFN Gruppo Collegato di Cosenza, Laboratori Nazionali di Frascati, Frascati, Italy. ¹⁶³Charles University, Faculty of Mathematics and Physics, Prague, Czech Republic. ¹⁶⁴TRIUMF, Vancouver, British Columbia, Canada. ¹⁶⁵SUPA – School of Physics and Astronomy, University of Edinburgh, Edinburgh, UK. ¹⁶⁶Departamento de Física, Universidade do Minho, Braga, Portugal. ¹⁶⁷Istanbul Bilgi University, Faculty of Engineering and Natural Sciences, Istanbul, Turkey. ¹⁶⁸Palacký University, RCPTM, Joint Laboratory of Optics, Olomouc, Czech Republic. ¹⁶⁹High Energy Physics Institute, Tbilisi State University, Tbilisi, Georgia. ¹⁷⁰Department of Physics, Nanjing University, Nanjing, China. ¹⁷¹Department of Physics, University of Pennsylvania, Philadelphia, PA, USA. ¹⁷²Physics Department, Tsinghua University, Beijing, China. ¹⁷³Department of Physics, Chinese University of Hong Kong, Shatin, Hong Kong. ¹⁷⁴Department of Physics, National Tsing Hua University, Hsinchu, Taiwan. ¹⁷⁵INFN Sezione di Lecce, Lecce, Italy. ¹⁷⁶School of Physics, University of the Witwatersrand, Johannesburg, South Africa. ¹⁷⁷University of Chinese Academy of Science (UCAS), Beijing, China. ¹⁷⁸Institute of Physics of the Czech Academy of Sciences, Prague, Czech Republic. ¹⁷⁹Department of Experimental Particle Physics, Jožef Stefan Institute and Department of Physics, University of Ljubljana, Ljubljana, Slovenia. ¹⁸⁰Dipartimento Politecnico di Ingegneria e Architettura, Università di Udine, Udine, Italy. ¹⁸¹LPSC, Université Grenoble Alpes, CNRS/IN2P3, Grenoble, France. ¹⁸²Instituto Superior Técnico, Universidade de Lisboa, Lisbon, Portugal. ¹⁸³Department of Physics, University of British Columbia, Vancouver, British Columbia, Canada. ¹⁸⁴Department of Physics, New York University, New York, NY, USA. ¹⁸⁵Institute of Frontier and Interdisciplinary Science and Key Laboratory of Particle Physics and Particle Irradiation (MOE), Shandong University, Qingdao, China. ¹⁸⁶Lehrstuhl für Experimentelle Physik IV, Technische Universität Dortmund, Dortmund, Germany. ¹⁸⁷Departamento de Física, Universidad de Buenos Aires, Buenos Aires, Argentina. ¹⁸⁸Department of Physics and Astronomy, York University, Toronto, Ontario, Canada. ¹⁸⁹Departamento de Física, Pontificia Universidad Católica de Chile, Santiago, Chile. ¹⁹⁰Universidade Federal de São João del Rei (UFSJ), São João del Rei, Brazil. ¹⁹¹Instituto de Física, Universidade de São Paulo, São Paulo, Brazil.

¹⁹²Department of Physics, University of Adelaide, Adelaide, South Australia, Australia. ¹⁹³Departamento de Física, Faculdade de Ciências, Universidade de Lisboa, Lisbon, Portugal. ¹⁹⁴National Centre for Scientific Research 'Demokritos', Agia Paraskevi, Greece. ¹⁹⁵INFN Sezione di Pavia, Pavia, Italy. ¹⁹⁶Dipartimento di Fisica, Università di Pavia, Pavia, Italy. ¹⁹⁷Physics Department, University of Texas at Dallas, Richardson, TX, USA. ¹⁹⁸Departamento de Física, Universidade de Coimbra, Coimbra, Portugal. ¹⁹⁹INFN-TIFPA, Trento, Italy. ²⁰⁰Università degli Studi di Trento, Trento, Italy. ²⁰¹Graduate School of Science and Technology, Tokyo Metropolitan University, Tokyo, Japan. ²⁰²Nagasaki Institute of Applied Science, Nagasaki, Japan. ²⁰³Enrico Fermi Institute, University of Chicago, Chicago, IL, USA. ²⁰⁴Institute for Theoretical and Experimental Physics named by A.I. Alikhanov of National Research Centre 'Kurchatov Institute', Moscow, Russia. ²⁰⁵Marian Smoluchowski Institute of Physics, Jagiellonian University, Krakow, Poland. ²⁰⁶D.V. Skobeltsyn Institute of Nuclear Physics, M.V. Lomonosov Moscow State University, Moscow, Russia. ²⁰⁷Dipartimento di Matematica e Fisica, Università del Salento, Lecce, Italy. ²⁰⁸Faculté des Sciences, Université Ibn-Tofail, Kénitra, Morocco. ²⁰⁹West University in Timisoara, Timisoara, Romania. ²¹⁰Department of Physics and Astronomy, University of New Mexico, Albuquerque, NM, USA. ²¹¹Institut für Astro- und Teilchenphysik, Leopold-Franzens-Universität, Innsbruck, Austria. ²¹²Division of Physics and Tomonaga Center for the History of the Universe, Faculty of Pure and Applied Sciences, University of Tsukuba, Tsukuba, Japan. ²¹³B.I. Stepanov Institute of Physics, National Academy of Sciences of Belarus, Minsk, Belarus. ²¹⁴Department of Physics, Shinshu University, Nagano, Japan. ²¹⁵Graduate School of Science, Kobe University, Kobe, Japan. ²¹⁶Graduate School of Science, Osaka University, Osaka, Japan. ²¹⁷Research Institute for Nuclear Problems of Byelorussian State University, Minsk, Belarus. ²¹⁸Physics Department, SUNY Albany, Albany, NY, USA. ²¹⁹E. Andronikashvili Institute of Physics, Iv. Javakishvili Tbilisi State University, Tbilisi, Georgia. ²²⁰Waseda University, Tokyo, Japan. ²²¹Research Center for Advanced Particle Physics and Department of Physics, Kyushu University, Fukuoka, Japan. ²²²Institute of Physics, Azerbaijan Academy of Sciences, Baku, Azerbaijan. ²²³Istanbul Aydin University, Application and Research Center for Advanced Studies, Istanbul, Turkey. ²²⁴Department of Physics, Universidad Andres Bello, Santiago, Chile. ²²⁵Instituto de Alta Investigación, Universidad de Tarapacá, Arica, Chile. ²²⁶Department of Physics and Institute for Advanced Study, Hong Kong University of Science and Technology, Clear Water Bay, Hong Kong. ²²⁷Department of Physics, University of Hong Kong, Hong Kong, China. ²²⁸Physics Department, Royal Institute of Technology, Stockholm, Sweden. ²²⁹Centro de Física Nuclear da Universidade de Lisboa, Lisbon, Portugal. ²³⁰Facultad de Ciencias y Centro de Investigaciones, Universidad Antonio Nariño, Bogotá, Colombia. ²³¹Faculty of Applied Information Science, Hiroshima Institute of Technology, Hiroshima, Japan. ²³²Transilvania University of Brasov, Brasov, Romania. ²³³National Institute for Research and Development of Isotopic and Molecular Technologies, Physics Department, Cluj-Napoca, Romania. ²³⁴Centre de Calcul de l'Institut National de Physique Nucléaire et de Physique des Particules (IN2P3), Villeurbanne, France. ²³⁵Departamento de Física, Universidad Nacional de Colombia, Bogotá, Colombia. ²³⁶Louisiana Tech University, Ruston, LA, USA. ²³⁷Division of Physics, TOBB University of Economics and Technology, Ankara, Turkey. ²³⁸Kyoto University of Education, Kyoto, Japan. ²³⁹Present address: Department of Physics, University of Fribourg, Fribourg, Switzerland. ²⁴⁰Present address: Departament de Física de la Universitat Autònoma de Barcelona, Barcelona, Spain. ²⁴¹Present address: Moscow Institute of Physics and Technology State University, Dolgoprudny, Russia. ²⁴²Present address: Department of Physics, Ben Gurion University of the Negev, Beer Sheva, Israel. ²⁴³Present address: Università di Napoli Parthenope, Naples, Italy. ²⁴⁴Present address: Institute of Particle Physics (IPP), Victoria, British Columbia, Canada. ²⁴⁵Present address: Department of Physics, St Petersburg State Polytechnical University, St Petersburg, Russia. ²⁴⁶Present address: Borough of Manhattan Community College, City University of New York, New York, NY, USA. ²⁴⁷Present address: Department of Physics, California State University, Fresno, CA, USA. ²⁴⁸Present address: Department of Financial and Management Engineering, University of the Aegean, Chios, Greece. ²⁴⁹Present address: Centro Studi e Ricerche Enrico Fermi, Rome, Italy. ²⁵⁰Present address: Department of Physics, California State University, East Bay, CA, USA. ²⁵¹Present address: Institutio Catalana de Recerca i Estudis Avancats, ICREA, Barcelona, Spain. ²⁵²Present address: Graduate School of Science, Osaka University, Osaka, Japan. ²⁵³Present address: Physikalisches Institut, Albert-Ludwigs-Universität Freiburg, Freiburg, Germany. ²⁵⁴Present address: University of Chinese Academy of Sciences (UCAS), Beijing, China. ²⁵⁵Present address: Institute of Physics, Azerbaijan Academy of Sciences, Baku, Azerbaijan. ²⁵⁶Present address: Institute for Mathematics, Astrophysics and Particle Physics, Radboud University/Nikhef, Nijmegen, Netherlands. ²⁵⁷Present address: CERN, Geneva, Switzerland. ²⁵⁸Present address: Joint Institute for Nuclear Research, Dubna, Russia. ²⁵⁹Present address: Hellenic Open University, Patras, Greece. ²⁶⁰Present address: The City College of New York, New York, NY, USA. ²⁶¹Present address: Dipartimento di Matematica, Informatica e Fisica, Università di Udine, Udine, Italy. ²⁶²Present address: Department of Physics, California State University, Sacramento, CA, USA. ²⁶³Present address: Département de Physique Nucléaire et Corpusculaire, Université de Genève, Geneva, Switzerland. ²⁶⁴Present address: Louisiana Tech University, Ruston, LA, USA. ²⁶⁵Present address: Institute for Nuclear Research and Nuclear Energy (INRNE) of the Bulgarian Academy of Sciences, Sofia, Bulgaria. ²⁶⁶Present address: Faculty of Physics, M.V. Lomonosov Moscow State University, Moscow, Russia. ²⁶⁷Present address: Institut für Experimentalphysik, Universität Hamburg, Hamburg, Germany. ²⁶⁸Present address: CPPM, Aix-Marseille Université, Marseille, France. ²⁶⁹Present address: National Research Nuclear University MEPhI, Moscow, Russia. ²⁷⁰Present address: Institute for Particle and Nuclear Physics, Wigner Research Centre for Physics, Budapest, Hungary. ²⁷¹Present address: Giresun University, Faculty of Engineering, Giresun, Turkey. ²⁷²Present address: Department of Physics and Astronomy, Michigan State University, East Lansing, MI, USA. ²⁷³Deceased: F. Bauer, O. Igonkina, D. Lellouch, A. Ouraou, V. Vrba, S. Zimmermann. ⁸²e-mail: atlas.publications@cern.ch